

# Clinically Relevant Basics of Pacing and Defibrillation

*T. Jared Bunch, David L. Hayes, Paul A. Friedman*

## Anatomy and physiology of the cardiac conduction system

The cardiac conduction system consists of specialized tissue involved in the generation and conduction of electrical impulses throughout the heart. In this book, we review how device therapy can be optimally utilized for various forms of conduction system disturbances, tachyarrhythmias, and for heart failure. Knowledge of the normal anatomy and physiology of the cardiac conduction system is critical to understanding appropriate utilization of device therapy.

The sinoatrial (SA) node, located at the junction of the right atrium and the superior vena cava, is normally the site of impulse generation (Fig. 1.1). The SA node is composed of a dense collagen matrix containing a variety of cells. The large, centrally located P cells are thought to be the origin of electrical impulses in the SA node, which is surrounded by transitional cells and fiber tracts extending through the perinodal area into the right atrium proper. The SA node is richly innervated by the autonomic nervous system, which has a key function in heart rate regulation. Specialized fibers, such as Bachmann's bundle, conduct the impulse throughout the right and left atria. The SA node has the highest rate of spontaneous depolarization and under normal circumstances is responsible for generating most impulses.

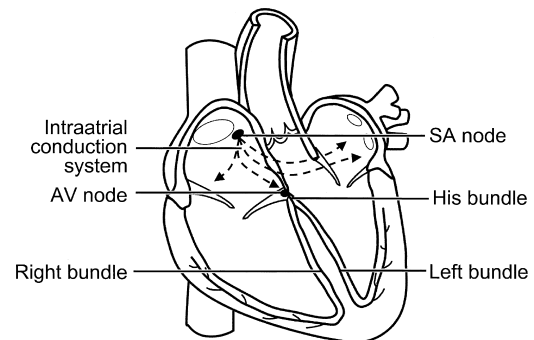


**Fig. 1.1** Drawing of the cardiac conduction system. AV, atrioventricular; SA, sinoatrial. See text for details.

Atrial conduction fibers converge, forming multiple inputs into the atrioventricular (AV) node, a small subendocardial structure located within the interatrial septum (Fig. 1.1). The AV node likewise receives abundant autonomic innervation, and it is histologically similar to the SA node because it is composed of a loose collagen matrix in which P cells and transitional cells are located. Additionally, Purkinje cells and myocardial contractile fibers may be found. The AV node allows for physiological delay between atrial and ventricular contraction, resulting in optimal cardiac hemodynamic function. It can also function as a subsidiary “pacemaker” should the SA node fail. Finally, the AV node functions (albeit typically suboptimally) to regulate the number of impulses eventually reaching the ventricle in instances of atrial tachyarrhythmia.

Purkinje fibers emerge from the distal AV node to form the bundle of His, which runs through the mem-

branous septum to the crest of the muscular septum, where it divides into the various bundle branches. The bundle branch system exhibits significant individual variation and is invariably complex. The right bundle is typically a discrete structure running along the right side of the interventricular septum to the anterior papillary muscle, where it divides. The left bundle is usually a large band of fibers fanning out over the left ventricle, sometimes forming functional fascicles. Both bundles eventually terminate in individual Purkinje fibers interdigitating with myocardial contractile fibers. The His-Purkinje system has little in the way of autonomic innervation.

Because of their key function and location, the SA and AV nodes are the most common sites of conduction system failure; it is therefore understandable that the most common indications for pacemaker implantation are SA node dysfunction and high-grade AV block. It should be noted, however, that conduction system disease is frequently diffuse and may involve the specialized conduction system at multiple sites.

Although the earliest pacemakers were designed to treat life-threatening ventricular bradyarrhythmias, indications have drastically expanded to include conditions that do not specifically involve intrinsic conduction system disease. Guidelines have been developed to provide uniform criteria for device implantation, but the importance of the patient's clinical status and any extenuating circumstances should also be considered.

## Electrophysiology of myocardial stimulation

Stimulation of the myocardium by a pacemaker re-

quires the initiation of a self-propagating wave of depolarization from the site of initial activation, whether from a native "pacemaker" or from an artificial stimulus. Myocardium exhibits a biological property referred to as "excitability," which is a response to a stimulus out of proportion to the strength of that stimulus.<sup>1</sup> Excitability is maintained by separation of chemical charge, which results in an electrical transmembrane potential. In cardiac myocytes, this electrochemical gradient is created by differing intracellular and extracellular concentrations of sodium ( $\text{Na}^+$ ) and potassium ( $\text{K}^+$ ) ions;  $\text{Na}^+$  ions predominate extracellularly and  $\text{K}^+$  ions predominate intracellularly. Although this transmembrane gradient is maintained by the high chemical resistance intrinsic to the lipid bilayer of the cellular membrane, passive leakage of these ions occurs across the cellular membrane through ion channels. Passive leakage is offset by two active transport mechanisms, each transporting three positive charges out of the myocyte in exchange for two positive charges that are moved into the myocyte, producing cellular polarization.<sup>2,3</sup> These active transport mechanisms require energy and are susceptible to disruption when energy-generating processes are interrupted.

The chemical gradient has a key role in the generation of the transmembrane action potential (Fig. 1.2). The membrane potential of approximately  $-90\text{ mV}$  drifts upward to the threshold potential of approximately  $-70$  to  $-60\text{ mV}$ . At this point, specialized membrane-bound channels modify their conformation from an inactive to an active state, which allows the abrupt influx of extracellular  $\text{Na}^+$  ions into the myocyte<sup>4,5</sup>, creating phase 0 of the action potential and rapidly raising the transmembrane potential to approximately  $+20\text{ mV}$ .<sup>6,7</sup>

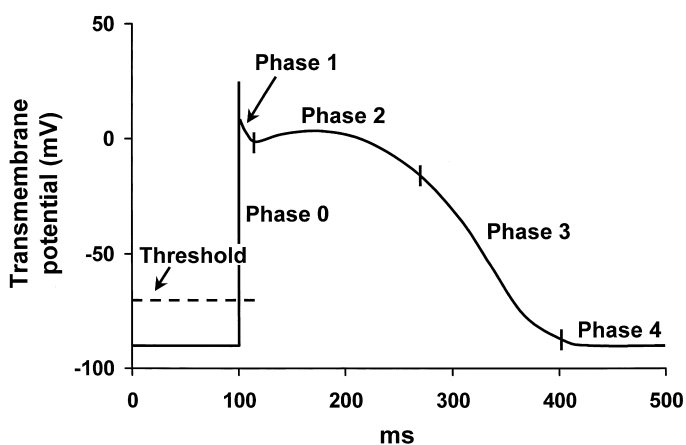


**Fig. 1.2** Action potential of a typical Purkinje fiber, with the various phases of depolarization and repolarization (described in the text). (From Stokes KB, Kay GN. Artificial electric cardiac stimulation. In: Ellenbogen KA, Kay GN, Wilkoff BL, eds. *Clinical cardiac pacing*. Philadelphia: WB Saunders Co., 1995:3–37. By permission of the publisher.)

This rapid upstroke creates a short period of overshoot potential (phase 1), which is followed by a plateau period (phase 2) created by the inward calcium ( $\text{Ca}^{2+}$ ) and  $\text{Na}^+$  currents balanced against outward  $\text{K}^+$  currents.<sup>8–10</sup> During phase 3 of the action potential, the transmembrane potential returns to normal, and during phase 4 the gradual upward drift in transmembrane potential repeats. The shape of the transmembrane potential and the relative distribution of the various membrane-bound ion channels differ between the components of the specialized cardiac conduction system.

Depolarization of neighboring cells occurs as a result of passive conduction via low-resistance intercellular connections called “gap junctions,” with active regeneration along cellular membranes.<sup>11,12</sup> The velocity of depolarization throughout the myocardium depends on the speed of depolarization of the various cellular components of the myocardium and on the geometrical arrangement and orientation of the myocytes. Factors such as myocardial ischemia, electrolyte imbalance, metabolic abnormalities, and drugs may affect the depolarization and depolarization velocity.

## Pacing basics

### Stimulation threshold

Artificial pacing involves delivery of an electrical impulse from an electrode of sufficient strength to cause depolarization of the myocardium in contact with that electrode and propagation of that depolarization to the rest of the myocardium. The minimal amount of energy required to produce this depolarization is called the

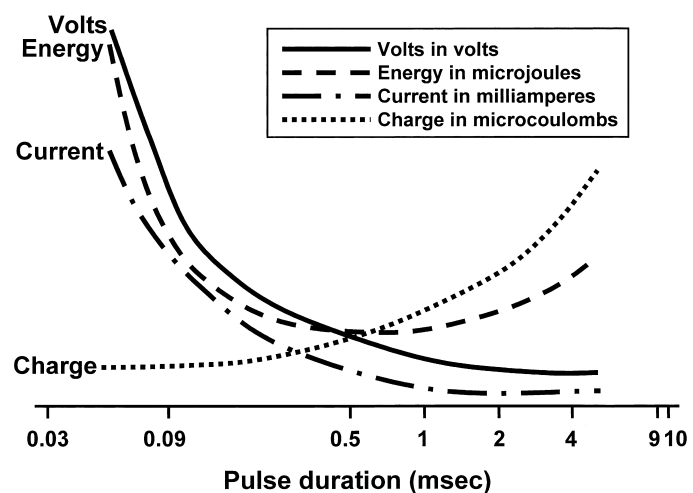
stimulation threshold. The components of the stimulus include the pulse amplitude (measured in volts) and the pulse duration (measured in milliseconds). An exponential relationship exists between the stimulus amplitude and the duration, resulting in a hyperbolic strength–duration curve. At short pulse durations, a small change in the pulse duration is associated with a significant change in the pulse amplitude required to achieve myocardial depolarization; conversely, at long pulse durations, a small change in pulse duration has relatively little effect on threshold amplitude (Fig. 1.3). Two points on the strength–duration curve should be noted (Fig. 1.4). The *rheobase* is defined as the smallest amplitude (voltage) that stimulates the myocardium at an infinitely long pulse duration (milliseconds). The *chronaxie* is the threshold pulse duration at twice the stimulus amplitude, which is twice the rheobase voltage. The chronaxie is important in the clinical practice of pacing because it approximates the point of minimum threshold energy (microjoules) required for myocardial depolarization.

The relationship of voltage, current, and pulse duration to stimulus energy is described by the formula

$$E = V^2/R \times t$$

in which  $E$  is the stimulus energy,  $V$  is the voltage,  $R$  is the total pacing impedance, and  $t$  is the pulse duration. This formula demonstrates the relative increase in energy with longer pulse durations. The energy increase due to duration is offset by a decrement in the needed voltage.

**Fig. 1.3** Relationship of charge, energy, voltage, and current to pulse duration. As the pulse duration is shortened, voltage and current requirements increase. Charge decreases as pulse duration shortens. At threshold, energy is lowest at a pulse duration of 0.5–1.0 ms and increases at pulse widths of shorter and longer duration. (Modified from Furman S. Basic concepts. In: Furman S, Hayes DL, Holmes DR Jr, eds. *A practice of cardiac pacing*. Mount Kisco, NY: Futura Publishing Co. By permission of the publisher.)



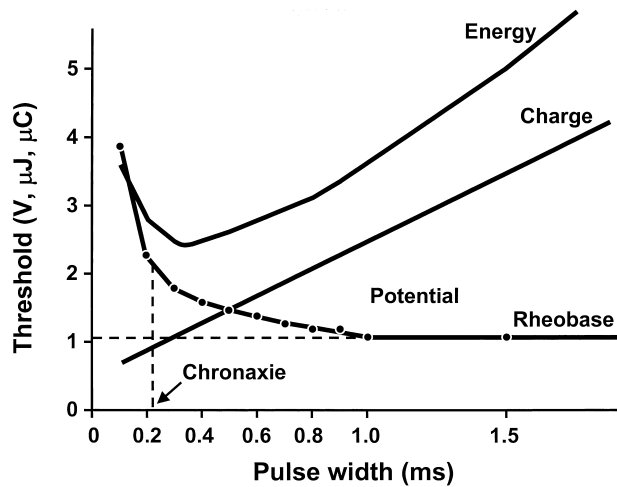


**Fig. 1.4** Relationships among chronic ventricular strength-duration curves from a canine, expressed as potential (V), charge ( $\mu\text{C}$ ), and energy ( $\mu\text{J}$ ). Rheobase is the threshold at infinitely long pulse duration. Chronaxie is the pulse duration at twice rheobase. (From Stokes K, Bornzin G. The electrode-biointerface stimulation. In: Barold SS, ed. *Modern cardiac pacing*. Mount Kisco, NY: Futura Publishing Co., 1985:33-77. By permission of the publisher.)

The strength-duration curve discussed thus far has been that of a constant voltage system, because contemporary permanent pacemakers are constant voltage systems. Constant current devices are no longer used (Fig. 1.5). It should be recognized, however, that constant current strength-duration curves can also be constructed.<sup>13</sup> These strength-duration curves, like constant voltage curves, are hyperbolic in shape, but they have a much more gradual decline in current requirements as the pulse width lengthens. Because of this gradual de-

cline, chronaxie of a constant current system is significantly greater than that in a constant voltage system.

Impedance is the term applied to the impediment to current flow in the pacing system. Ohm's law describes the relationship among voltage, current, and resistance as

$$V = IR$$

in which  $V$  is the voltage,  $I$  is the current, and  $R$  is the resistance. Although Ohm's law is used for determining impedance, technically impedance and resistance are not interchangeable terms. Impedance implies inclusion of all factors that contribute to current flow impediment, including lead conductor resistance, electrode resistance, resistance due to electrode polarization, capacitance and inductance. Technically, the term "resistance" does not include the effects of capacitance (storage of charge) or inductance (storage of current flow) to impede current flow. Nevertheless, Ohm's law (substituting impedance for  $R$ ) is commonly used for calculating impedance. In constant voltage systems, the lower the pacing impedance, the greater the current flow; conversely, the higher the pacing impedance, the lower the current flow. Ideally, the lead conductor material would have a low resistance to minimize the generation of energy-wasting heat as the current flows along the lead, and the electrode would have a high resistance to minimize current flow and negligible electrode polarization. Decreasing the electrode radius minimizes current

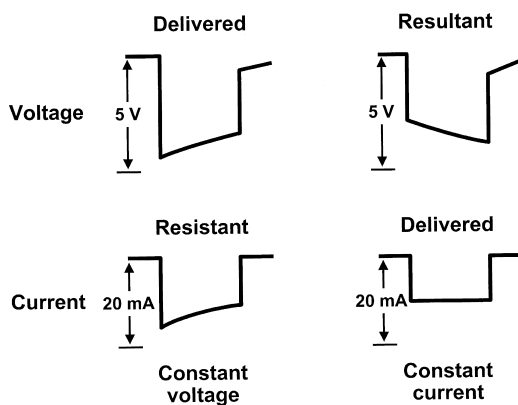


**Fig. 1.5** Diagrammatic representation of the delivered voltage and resultant current in a constant-voltage system compared with the delivered current and resultant voltage in a constant-current system. (Modified from Stokes K, Bornzin G. The electrode-biointerface stimulation. In: Barold SS, ed. *Modern cardiac pacing*. Mount Kisco, NY: Futura Publishing Co., 1985:33-77. By permission of the publisher.)

flow by providing greater electrode resistance and increased current density, resulting in greater battery longevity and lower stimulation thresholds.<sup>14</sup>

“Polarization” refers to layers of oppositely charged ions that surround the electrode during the pulse stimulus. It is related to the movement of positively charged ions ( $\text{Na}^+$  and  $\text{H}_3\text{O}^+$ ) to the cathode; the layer of positively charged ions is then surrounded by a layer of negatively charged ions ( $\text{Cl}^-$ ,  $\text{HPO}_4^{2-}$ , and  $\text{OH}^-$ ). These layers of charge develop during the pulse stimulus, reaching peak formation at the termination of the pulse stimulus, after which they gradually dissipate. Polarization impedes the movement of charge from the electrode to the myocardium, resulting in a need for increased voltage. Since polarization develops with increasing pulse duration, one way to combat formation of polarization is to shorten the pulse duration. Electrode design has incorporated the use of materials that discourage polarization, such as platinum black, iridium oxide, titanium nitride, and activated carbon.<sup>15</sup> Finally, polarization is inversely related to the surface area of the electrode. To maximize the surface area (to reduce polarization) but minimize the radius (to increase electrode impedance), electrode design incorporates a small radius but a porous, irregular surface construction.<sup>16</sup> Leads designed to maximize these principles are considered “high-impedance” leads.

### Variations in stimulation threshold

Myocardial thresholds typically fluctuate, occasionally dramatically, during the first weeks after implantation. After implantation of earlier generations of endocardial leads, the stimulation threshold would typically rise rapidly in the first 24 h and then gradually increase to a peak at approximately 1 week (Fig. 1.6). Over the ensuing 6–8 weeks, the stimulation threshold would usually decline to a level somewhat higher than that at implantation, but less than the peak threshold, known as the “chronic threshold”.<sup>17,18</sup> The magnitude and duration of this early increase in threshold is highly dependent on lead design, the interface between the electrode and the myocardium, and individual patient variation, but chronic thresholds would typically be reached by 3 months. The single most important lead design change to alter pacing threshold evolution was incorporation of steroid elution at the lead tip. With steroid elution there is a slight increase in thresholds post implantation, with subsequent reduction to almost that of acute thresholds.<sup>19,20</sup>

Transvenous pacing leads have used passive or active fixation mechanisms to provide a stable electrode–myocardium interface. Active fixation leads may have higher initial pacing thresholds at implantation, but frequently decline significantly within the first 5–30 min after placement.<sup>17</sup> This effect has been at-

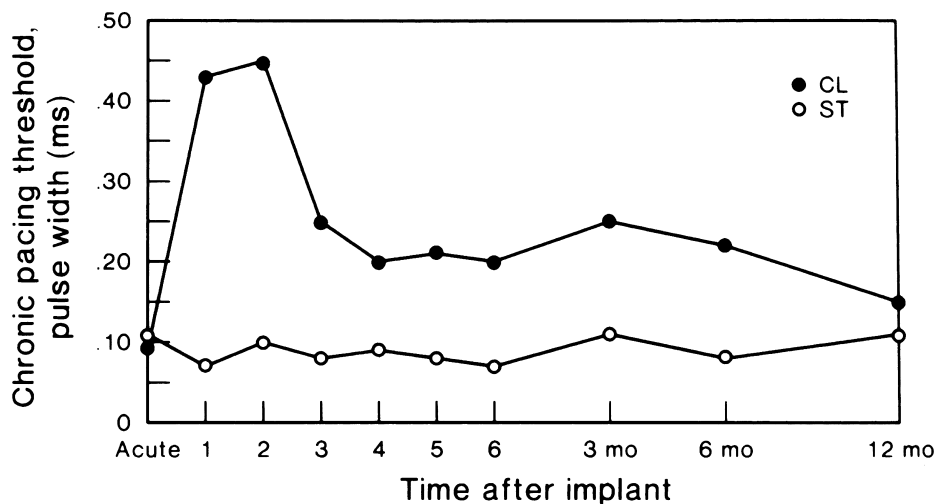


**Fig. 1.6** Long-term pacing thresholds from a conventional lead (no steroid elution) (CL; closed circles) and a steroid-eluting lead (ST; open circles). With the conventional lead, an early increase in threshold decreases to a plateau at approximately 4 weeks. The threshold for the steroid-eluting lead remains relatively flat, with no significant

change from short-term threshold measurements. (From Furman S. Basic concepts. In: Furman S, Hayes DL, Holmes DR Jr, eds. *A practice of cardiac pacing*, second edn. Mount Kisco, NY: Futura Publishing Co., 1989:23–78. By permission of Mayo Foundation.)

tributed to hyperacute injury due to advancement of the screw into the myocardium. On a cellular level, implantation of a transvenous pacing lead results in acute injury to cellular membranes, which is followed by the development of myocardial edema and coating of the electrode surface with platelets and fibrin. Subsequently, various chemotactic factors are released, and an acute inflammatory reaction develops, consisting of mononuclear cells and polymorphonuclear leukocytes. After the acute response, release of proteolytic enzymes and oxygen free radicals by invading macrophages accelerates cellular injury. Finally, fibroblasts in the myocardium begin producing collagen, leading to production of the fibrotic capsule surrounding the electrode. This fibrous capsule ultimately increases the effective radius of the electrode, with a smaller increase in surface area.<sup>21,22</sup> Steroid-eluting leads are believed to minimize fibrous capsule formation. In both atrial and ventricular active fixation leads, steroid elution results in long-term reduction in energy consumption with maintenance of stimulation thresholds, lead impedance values, and sensing thresholds.<sup>23,24</sup>

The stimulation threshold typically has a circadian pattern, generally increasing during sleep and decreasing during the day, probably reflecting changes in autonomic tone. The stimulation threshold may also rise after eating; during hyperglycemia, hypoxemia or acute viral illnesses; or as a result of electrolyte fluctuations. These changes, as well as the circadian variation in stimulation threshold, are usually minimal. Certain drugs used in patients with cardiac disease may also increase pacing thresholds (see Chapter 8: Programming).

The inflammatory reaction and subsequent fibrosis that occur after lead implantation may act as an insulating shield around the electrode. These processes effectively increase the distance between the electrode and the excitable tissue, allowing the stimulus to disperse partially before reaching the excitable cells. These changes result in an increased threshold for stimulation and attenuate the amplitude and slew rate of the endocardial signal being sensed. This is a process termed “lead maturation.” Improvements in electrode design and materials have reduced the severity of the inflammatory reaction and thus improved lead maturation rates.<sup>19,25</sup> When the capture threshold exceeds the programmed output of the pacemaker, exit block will occur; loss of capture will result if the capture threshold exceeds the programmed output of the pacemaker.<sup>17,26</sup> Exit block, a consequence of lead matu-

ration, results from the progressive rise in thresholds over time.<sup>17,26</sup> This phenomenon occurs despite initial satisfactory lead placement and implantation thresholds, often but not always occurs in parallel in the atrium and ventricle, and usually recurs with placement of subsequent leads. Steroid-eluting leads prevent exit block in most, but not all patients (Fig. 1.7).

### Sensing

The first pacemakers functioned as fixed-rate, VOO devices. All contemporary devices offer demand-mode pacing, which pace only when the intrinsic rate is below the programmed rate. For such devices to function as programmed, accurate and consistent sensing of the native rhythm was essential.

Intrinsic cardiac electrical signals are produced by the wave of electrical current through the myocardium (Fig. 1.8). As the wavefront of electrical energy approaches an endocardial electrode, the electrode becomes positively charged relative to the depolarized region, recorded as a positive deflection in the intracardiac electrogram. As the wavefront passes directly under the electrode, the outside of the cell abruptly becomes negatively charged, and a sharp negative deflection is recorded, which is referred to as the intrinsic deflection.<sup>27</sup> It is considered to occur at the moment the advancing wavefront passes directly underneath the electrode. Smaller positive and negative deflections preceding and following the intrinsic deflection represent activation of surrounding myocardium. Ventricular electrograms typically are much larger than atrial electrograms because the ventricular mass is greater. The maximum frequency densities of atrial and ventricular electrograms have generally been found to be in the range of 80–100 Hz in the atrium and 10–30 Hz in the ventricle (these frequencies may differ slightly with newer leads/technologies). Based on these frequencies, filtering systems of pulse generators were designed to attenuate signals outside these ranges. Filtering and use of blanking and refractory periods have markedly reduced unwanted sensing, although myopotential frequencies (ranging from 10 to 200 Hz) considerably overlap with those generated by atrial and ventricular depolarization and are difficult to filter out, especially during sensing in a unipolar configuration.<sup>28–30</sup> Shortening of the tip-to-ring spacing has also improved atrial sensing and rejection of far-field R waves.

Another component of the intracardiac electrogram is the slew rate, i.e. the peak slope of the devel-

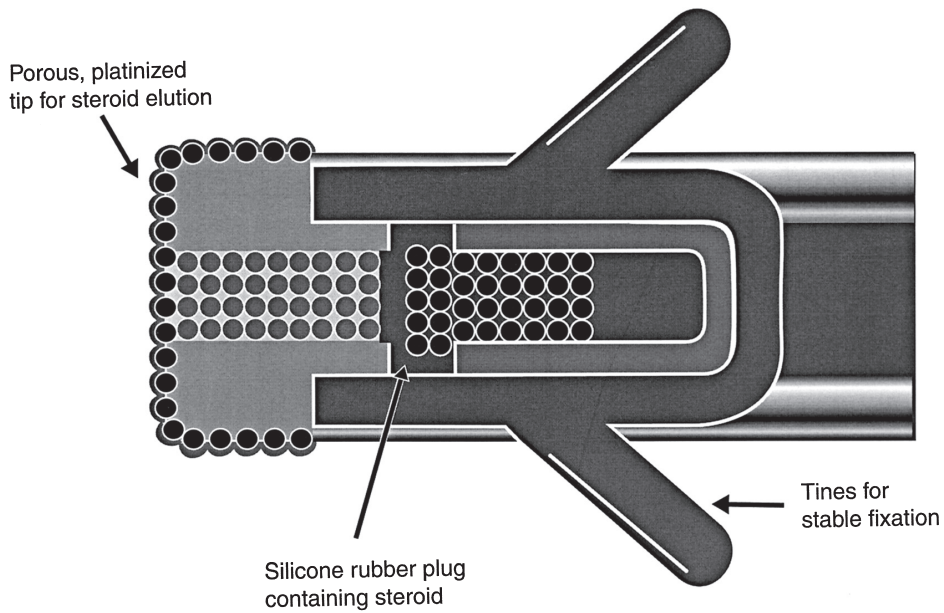


**Fig. 1.7** Diagram of a steroid-eluting passive fixation lead. The electrode has a porous, platinized tip. A silicone rubber plug is impregnated with 1 mg of dexamethasone sodium.

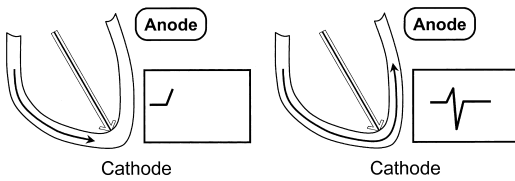


**Fig. 1.8** Schema of the relationship of the pacing lead to the recorded electrogram with unipolar sensing. Left, As the electrical impulse moves toward the cathode (lead tip), a positive deflection is created in the electrogram. Right, As the electrical impulse passes the cathode, the deflection suddenly becomes downward, and as the impulse moves away from the cathode, a negative deflection occurs.

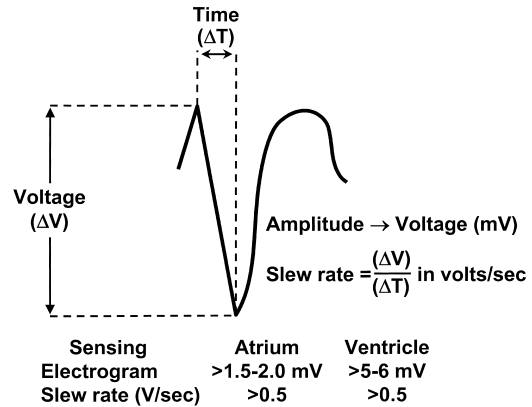


**Fig. 1.9** In the intracardiac electrogram, the difference in voltage recorded between two electrodes is the amplitude, which is measured in millivolts. The slew rate is volts per second and should be at least 0.5.

oping electrogram<sup>31</sup> (Fig. 1.9). The slew rate represents the maximal rate of change of the electrical potential between the sensing electrodes and is the first derivative of the electrogram ( $dV/dt$ ). An acceptable slew rate should be at least 0.5V/s in both the atrium and the ventricle. In general, the higher the slew rate, the higher the frequency content and the more likely the signal will be sensed. Slow, broad signals, such as those generated by the T wave, are much less likely to be sensed because of a low slew rate and lower frequency density.

Polarization also affects sensing function. After termination of the pulse stimulus, an excess of positive

charge surrounds the cathode, which then decays until electrically neutral. Afterpotentials can be sensed with inappropriate inhibition or delay of the subsequent pacing pulse (Fig. 1.10). The amplitude of afterpotentials is directly related to both the amplitude and the duration of the pacing pulse; thus, they are most likely to be sensed when the pacemaker is programmed to high voltage and long pulse duration in combination

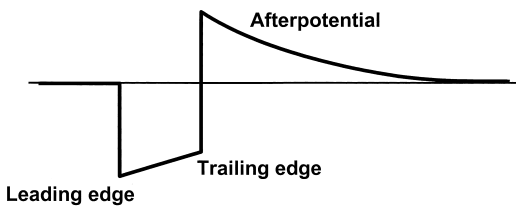


**Fig. 1.10** Diagram of a pacing pulse, constant-voltage, with leading edge and trailing edge voltage and an afterpotential with opposite polarity. As described in the text, afterpotentials may result in sensing abnormalities.

with maximal sensitivity.<sup>31</sup> The use of programmable sensing refractory and blanking periods has helped to prevent the pacemaker from reacting to afterpotentials, although in dual-chamber systems, atrial afterpotentials of sufficient strength and duration to be sensed by the ventricular channel may result in inappropriate ventricular inhibition (crosstalk), especially in unipolar systems.<sup>32,33</sup> Afterpotentials may be a source of problems in devices with automatic threshold measurement and capture detection; the use of leads designed to minimize afterpotentials may increase the effectiveness of such algorithms.<sup>34</sup>

“Source impedance” is a term used to describe the voltage drop that occurs from the site of the origin of the intracardiac electrogram to the proximal portion of the lead.<sup>35</sup> Components include the resistance between the electrode and the myocardium, the resistance of the lead conductor material, and the effects of polarization. The resistance between the electrode and the myocardium, as well as polarization, is inversely related to the surface area of the electrode; thus, the effects of both can be minimized by a large electrode surface area. The electrogram actually seen by the pulse generator is determined by the ratio between the sensing amplifier (input impedance) and the lead (source impedance). Less attenuation of the signal from the myocardium occurs when there is a greater ratio of input impedance to source impedance. Clini-

cally, impedance mismatch is seen with insulation or conductor failure, which results in sensing abnormalities or failure.

## Lead design

Pacing lead components include the electrode and fixation device, the conductor, the insulation, and the connector pin (Figs 1.11 and 1.12). Leads function in a harsh environment *in vivo*. They must be constructed of materials that provide both mechanical stability and flexibility; they must have satisfactory electrical conductive and resistive properties; the insulating material must be durable but ideally have a low friction coefficient to facilitate implantation; and the electrode must provide good mechanical and electrical contact with the myocardium. Industry continues to modify and improve lead design, but the “ideal” lead remains a constant goal.

As previously discussed, optimal stimulation and sensing thresholds favor an electrode with a small radius and a large surface area. Electrode shape and surface composition have evolved over time. Early models utilized a round spherical shape with a smooth metal surface. Electrodes with an irregular, textured surface allow for increased surface area without an increase in electrode radius.<sup>16,34,36</sup> To achieve increased electrode surface area, manufacturers have used a variety of designs, including microscopic pores, coatings of microspheres, and wire filament mesh.

Unfortunately, relatively few conductive materials have proven to be satisfactory for use in pacing electrodes. Ideally, electrodes are biologically inert, resist degradation over time, and do not elicit a marked tissue reaction at the myocardium–electrode interface. Certain metals, such as zinc, copper, mercury, nickel, lead and silver, are associated with toxic reactions with the myocardium. Stainless steel alloys are susceptible to corrosion. Titanium, tantalum, platinum and iridium oxide acquire a surface coating of

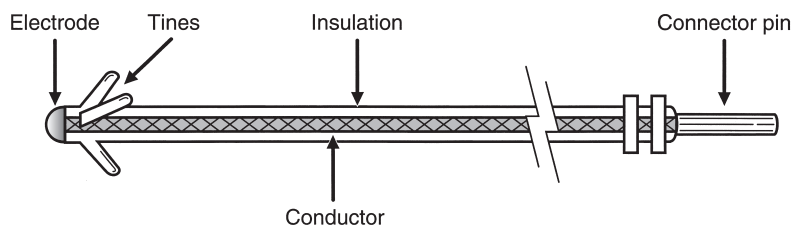


**Fig. 1.11** Basic components of a passive fixation pacing lead with tines.



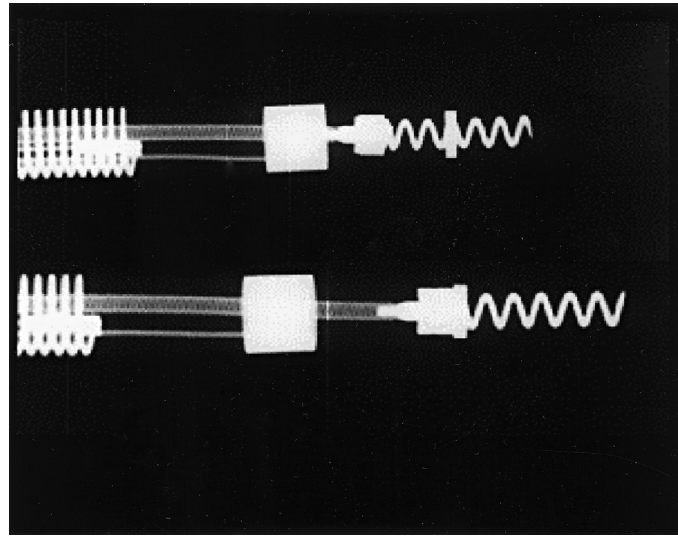


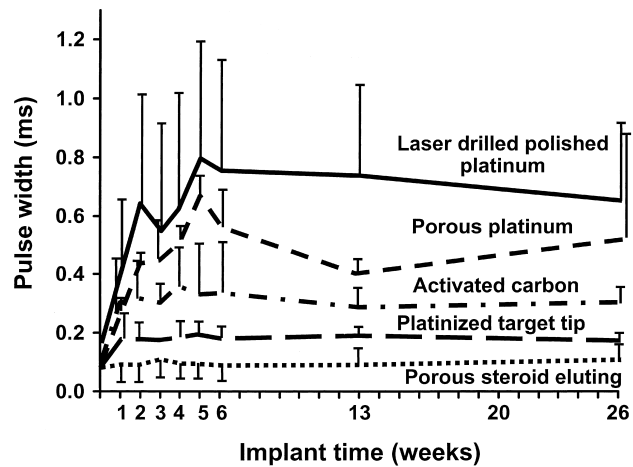
**Fig. 1.12** Radiographic example of an active fixation screw-in lead with a retractable screw rather than a screw that is always extended. The screw is extended in the lower image but not in the upper image.

oxides that impedes current transfer. Materials currently in use are platinum-iridium, platinized titanium-coated platinum, iridium oxide, and platinum (Fig. 1.13). Carbon electrodes seem to be least susceptible to corrosion; they have also been improved by a process known as activation, which roughens the surface to increase the surface area and allow for tissue ingrowth.<sup>37</sup>

Lead fixation may be active or passive. Passive fixation endocardial leads usually incorporate tines at the tip that become ensnared in trabeculated tissue in the right atrium or ventricle, providing lead stability. Leads designed for coronary venous placement usually incorporate a design that wedges the lead against

the wall of the coronary vein. Active fixation leads almost exclusively utilize screw mechanisms to embed in the myocardium to provide lead stability. Some leads incorporate screws that are electrically inactive, and in others the screw is electrically active. There are advantages and disadvantages to each design, and the clinical situation and preference of the operator are important considerations when a lead is chosen. Considerable myocardial and fibrous tissue enveloping the tip typically develops with both active and passive fixation leads. However, the encasement of the tines of a passive fixation lead by fibrous tissue often makes the extraction of passive fixation leads more difficult than that of active fixation leads. Active fixation leads are

**Fig. 1.13** Capture thresholds from implantation to 26 weeks from a variety of unipolar leads with similar geometric surface area electrodes. From top to bottom, the curves represent laser-drilled polished platinum; porous-surface platinum; activated carbon; platinized target tip; and porous steroid-eluting leads. (From Stokes KB, Kay GN. Artificial electric cardiac stimulation. In: Ellenbogen KA, Kay GN, Wilkoff BL, eds. *Clinical cardiac pacing*. Philadelphia: WB Saunders Co., 1995:3–37. By permission of the publisher.)



often preferable in patients with distorted anatomy, such as those with congenital cardiac defects or those with surgically amputated atrial appendages. Active fixation leads are also preferable in patients with high right-sided pressures. As alternative site pacing has evolved, i.e. the placements of leads outside the right atrial appendage and right ventricular apex, screw-in leads have become more popular and necessary for long-term stability.

There are various types of mechanism used to keep the screw unexposed until it is placed in an optimal site for fixation. One example is a system in which the screw is extendable and retractable from the pacemaker lead tip. This allows the operator to designate the precise location and timing to extend the screw from the tip. Another example involves covering a fixed helix screw in a material that dissolves in the blood stream in a time period that is advantageous for lead positioning. For example, screws can be covered by a mannitol compound that dissolves over time in the blood stream. Since the mannitol covers the screw, it prevents it from catching on tissue, allowing easier lead placement.

New technologies have emerged to assist in the placement of leads to targeted anatomical sites. Catheter-delivered systems use a deflectable catheter that is braided to allow the simultaneous ability to torque the catheter. A second technology developed to reach difficult anatomical targets is to use an over-the-wire lead delivery system, mainly used with placement of coronary venous leads for left ventricular stimulation. With this system the lead can be advanced to a stable position, a guidewire then being advanced to navigate tortuous regions similar to techniques used extensively for coronary angiography, followed by advancement of the lead over the wire. This approach not only improves access to target sites, but decreases injury to coronary venous structures. By combining these technologies, access to target sites has improved greatly, in particular, coronary vein subselection for left ventricular lead placement.

Conductors are commonly of a multifilament design to facilitate tensile strength and reduce resistance to metal fatigue (Fig. 1.14). Alloys such as MP35N (cobalt, nickel, chromium and molybdenum) and nickel-silver are typically used in modern pacing leads. Bipolar leads may be of coaxial design, with an inner coil extending to the distal electrode and an outer coil terminating at the proximal electrode (Fig. 1.15) This design requires that the conductor coils be separated

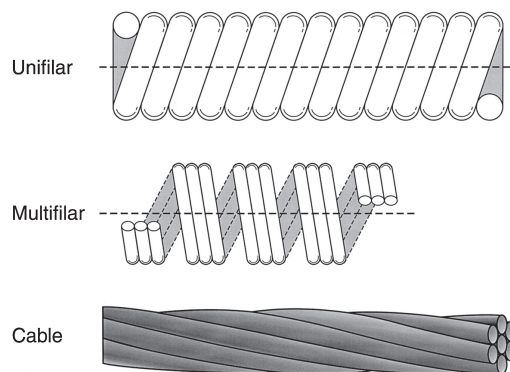


**Fig. 1.14** Conductor coils may be of unifilar, multifilar, or cable design. The multifilar and cable designs allow the conductor to be more flexible and more resistant to fracture.

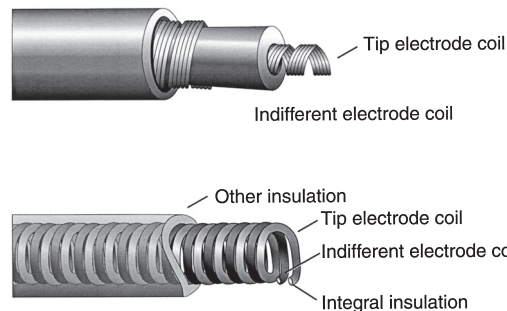


**Fig. 1.15** Varieties of conductor construction. Top, bipolar coaxial design with an inner multifilar coil surrounded by insulation (inner), an outer multifilar coil, and outer insulation. Bottom, individually coated wires wound together in a single multifilar coil for bipolar pacing.

by a layer of inner insulation. Coaxial designs remain commonly used in the treatment of bradyarrhythmias. Some bipolar leads are coradial, or “parallel-wound”; that is, two insulated coils are wound next to each other. Leads may also be constructed with the conductor coils parallel to each other (multiluminal), again separated by insulating material (Fig. 1.16). This type of design is typically used for tachyarrhythmia leads. Additionally, leads may use a combination of coils and cables. The coil facilitates the passage of a stylet for lead implantation, and the cable allows a smaller lead body.

Two materials have predominated in lead insulation: silicone and polyurethane. Each has its respective advantages and disadvantages, but the overall performance of both materials has been excellent.<sup>38</sup> Table 4.2 in

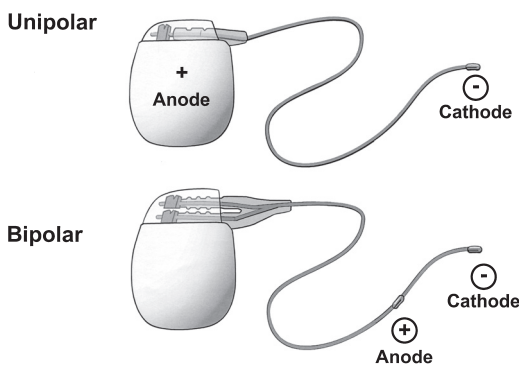


**Fig. 1.16** In a unipolar configuration, the pacemaker case serves as the anode, or (+), and the electrode lead tip as the cathode, or (-). In a bipolar configuration, the anode is located on the ring, often referred to as the “ring electrode,” proximal to the tip, or cathode. The distance between tip and ring electrode varies among manufacturers and models.

Chapter 4 compares the advantages and disadvantages of these two insulating materials.

The two grades of polyurethane that have had the widest use are Pellathane 80A and Pellathane 55D. Early after the introduction of polyurethane as an insulating material, it became clear that clinical failure rates with specific leads were higher than acceptable; further investigation revealed that the failures were occurring primarily in leads insulated with the P80A polymer.<sup>36,39</sup> Microscopic cracks developed in the P80A polymer, initially occurring as the heated polymer cooled during manufacture; with additional environmental stress, these cracks propagated deeper into the insulation, resulting in failure of the lead insulation.

Polyurethane may also undergo oxidative stress in contact with conductors containing cobalt and silver chloride, resulting in degradation of the lead from the inside and subsequent lead failure. Some current leads use silicone with a polyurethane coating, incorporating the strength and durability of silicone with the ease of handling of polyurethane while maintaining a satisfactory external lead diameter. Silicone rubber is well known to be susceptible to abrasion wear, cold flow due to cyclic compression, and wear from lead-to-lead and lead-to-can contact. Current silicone leads have surface modifications that improve lubricity and reduce friction in blood. Second, preliminary studies have suggested that a hybrid coating of silicone and polyurethane may offer improved wear.<sup>40</sup> Despite

lead improvements, laboratory testing and premarketing, clinical trials have been inadequate to predict the long-term performance of leads, so that clinicians implanting the devices or performing follow-up in patients with pacing systems must vigilantly monitor lead status.

Contemporary leads and connectors are standardized to conform to international guidelines (IS-1 Standard), which mandate that leads have a 3.2-mm diameter in-line bipolar connector pin.<sup>41</sup> These standards were established many years ago because some leads and connector blocks were incompatible, requiring the development of multiple adaptors. Some patients who have functioning leads of the older 5- or 6-mm diameter unipolar design require lead adaptors when the pulse generator is replaced.

Coronary venous lead connectors were initially developed to accommodate patients with heart failure who had previously implanted pacemakers for other reasons and were considered eligible for an upgrade to biventricular pacing. For these patients, the ventricular output of the pacemaker generator was divided via a “Y” connector from one bipolar output to two separate outputs (usually a unipolar left ventricle and a bipolar right ventricle or a bipolar left ventricle and a bipolar right ventricle) to accommodate the left ventricular lead. However, this approach can lead to atrial oversensing, improper measurement of left ventricular thresholds, and inappropriate shocks.<sup>42,43</sup> Currently, most left ventricular leads are connected to the pacemaker independently. The left ventricular leads are either bipolar or unipolar with a steroid eluting tip.

### Bipolar vs. unipolar pacing and sensing

In unipolar pacing systems, the lead tip functions as the cathode and the pulse generator functions as the anode (Fig. 1.16). In bipolar systems, the lead tip functions as the cathode and the lead ring functions as the anode (Fig. 1.16). Unipolar leads are of simpler design and have a smaller external diameter. Unipolar leads have historically demonstrated greater durability than bipolar leads. In recent years the difference in durability has been less distinct. Unipolar leads do not offer the option of bipolar function. Although unipolar and bipolar leads are readily available, present usage of transvenous leads is almost exclusively bipolar in the USA. This is in contrast to epicardial leads, of which there is a lower percentage of bipolar leads in use. Bipolar leads may function in the unipolar mode if the pace-

maker is so programmed. They are available in several designs, generally coaxial or multiluminal. Regardless of design, the external diameter of a bipolar lead is usually greater than that of unipolar leads because each coil must be electrically separated by insulating material. Bipolar pacing and sensing are preferred over unipolar because bipolar pacing cannot cause extracardiac stimulation at the pulse generator, which may occasionally occur with unipolar pacing due to current returning to the generator. Also, bipolar sensing is less likely to detect myopotentials, far-field signals and electromagnetic interference.<sup>44</sup>

There are long-standing controversies regarding unipolar vs. bipolar pacing and sensing configuration and which, if either, are superior.<sup>44</sup> Advocates of unipolar configuration argue that improvements in sensing circuitry and pacemaker filtering capabilities have minimized unipolar oversensing of extracardiac signals. The design of unipolar leads is often more simple and therefore the lead size may be less. They also argue that bipolar leads have a historically higher failure rate than unipolar leads. Although this is true, if the specific failures of Pellathane 80A and 55D that occurred many years ago are removed from the analysis, the failure rate between unipolar and bipolar lead designs does not differ significantly and varies between different manufacturers.<sup>45</sup> Unipolar leads are often considered safer because they do not short circuit significantly when there are insulation breaches, although they may be susceptible to significant external interference. Nevertheless, a lead that is malfunctioning in the bipolar mode may function satisfactorily when programmed to the unipolar configuration (see Chapter 8: Programming).

Most pulse generators offer independently programmable pacing and sensing in each channel; however, bipolar programming of a device attached to a unipolar lead results in no output. Bipolar leads can function in the unipolar mode; the converse is not true.

### Left ventricular leads

Cardiac resynchronization therapy with biventricular pacing is an established treatment for patients with severe congestive heart failure, low left ventricular ejection fraction, and New York Heart Association class III or IV heart failure.<sup>46</sup> In order to pace the left ventricle, a pacing lead is implanted transvenously through the coronary sinus and coronary vein to stimulate the left ventricular free wall. Resynchronization is obtained by stimulating both ventricles to contract with mini-

mal intraventricular delay, thereby improving the left ventricular performance.<sup>47</sup> Modifications of the tip geometry have improved the stability of the passive lead over time. Tissue ingrowth can be a major impediment to the removal of defibrillation leads implanted in the coronary sinus. Coating these leads with polytetrafluoroethylene and backfilling the coil with medical adhesive facilitates transvenous lead removal.<sup>48</sup>

### Pulse generators

All pulse generators include a power source, an output circuit, a sensing circuit, a timing circuit, and a header with a standardized connector (or connectors) to attach a lead (or leads) to the pulse generator.<sup>49</sup> Essentially, all devices are capable of storing some degree of diagnostic information that can be retrieved at a later time. Most pacemakers incorporate a rate-adaptive sensor. Despite increasing complexity, device size has continued to decrease. This has led to a variable effect on the potential longevity.

Many power sources have been used for pulse generators over the years. Lithium iodine cells have been the energy source for almost all contemporary pulse generators. Newer pacemakers and implantable cardioverter-defibrillators (ICDs) that can support higher current drains for capacitor charging and high-rate antitachycardia pacing use lithium-silver-oxide-vanadium chemistries. Lithium is the anodal element and provides the supply of electrons; iodine is the cathodal element and accepts the electrons. The cathodal and anodal elements are separated by an electrolyte, which serves as a conductor of ionic movement but a barrier to the transfer of electrons. The circuit is completed by the external load, i.e. the leads and myocardium. The battery voltage of the cell depends on the chemical composition of the cell; at the beginning of life for the lithium iodine battery, the cell generates approximately 2.8V, which decreases to 2.4V when approximately 90% of the useable battery life has been reached. The voltage then exponentially declines to 1.8V as the battery reaches end-of-life. However, the voltage at which the cell reaches a certain depth of discharge is load dependent. The elective replacement indicated voltages were chosen based on the shape of the discharge curves under expected operating conditions. When the battery is at end-of-service, most devices lose telemetry and programming capabilities, frequently reverting to a fixed high-output mode to attempt to maintain

patient safety. This predictable depletion characteristic has made lithium-based power cells common in current devices. Nickel-cadmium technology is being used once again in at least one investigational implantable device.

The battery voltage can be telemetered from the pulse generator; most devices also provide battery impedance (which increases with battery depletion) for additional information about battery life. The battery life can also be estimated by the magnet rate of the device, which changes with a decline in battery voltage. Unfortunately, the magnet rates are not standardized, and rate change characteristics vary tremendously among manufacturers and even among devices produced by the same manufacturer. Therefore, it is important to know the magnet rate characteristics of a given device before using this feature to determine battery status.

The longevity of any battery is determined by several factors, including chemical composition of the battery, size of the battery, external load (pulse duration and amplitude, stimulation frequency, total pacing lead impedance, and amount of current required to operate device circuitry and store diagnostic information), amount of internal discharge, and voltage decay characteristics of the cell. The basic formula for longevity determination is  $114 \times [\text{battery capacity (A-HR)} / \text{Current Drain } (\mu\text{A})] = \text{longevity in years}$ . However, this formula is subject to how the power cell's ampere-hours is specified by the manufacturer, thus the longevity will vary somewhat by company. High-performance leads, automatic capture algorithms and programming options that minimize pacing should further enhance device longevity.<sup>50,51</sup>

The pacing pulse is generated first by charging of an output capacitor and discharge of the capacitor to the pacing cathode and anode. Since the voltage of a lithium iodine cell is fixed, obtaining multiple selectable pulse amplitudes requires the use of a voltage amplifier between the battery and the output capacitor. Contemporary pulse generators are constant-voltage (rather than constant-current) devices, implying delivery of a constant-voltage pulse throughout the pulse duration. In reality, some voltage drop occurs between the leading and the trailing edges of the impulse; the size of this decrease depends on the pacing impedance and pulse duration. The lower the impedance, the greater the current flow from the fixed quantity of charge on the capacitor and the greater the voltage drop throughout the pulse duration.<sup>52</sup> The voltage drop is also depend-

ent on the capacitance value of the capacitor and the time of longer pulse duration.

The output waveform is followed by a low-amplitude wave of opposite polarity, the afterpotential. The afterpotential is determined by the polarization of the electrode at the electrode-tissue interface; formation is due to electrode characteristics as well as to pulse amplitude and duration. The sensing circuit may sense afterpotentials of sufficient amplitude, especially if the sensitivity threshold is low. Newer pacemakers use the output circuit to discharge the afterpotential quickly, thus lowering the incidence of afterpotential sensing. The afterpotential also helps to prevent electrode corrosion.

The intracardiac electrogram is conducted from the myocardium to the sensing circuit via the pacing leads, where it is then amplified and filtered. As noted above, the input impedance must be significantly larger than the sensing impedance to minimize attenuation of the electrogram. A bandpass filter attenuates signals on either side of a center frequency, which varies among manufacturers (generally ranging from 20 to 40 Hz).<sup>53,54</sup> After filtering, the electrogram signal is compared with a reference voltage, the sensitivity setting; signals with an amplitude of this reference voltage or higher are sensed as true intracardiac events and are forwarded to the timing circuitry, whereas signals with an amplitude below the reference amplitude are categorized as noise, extracardiac or other cardiac signal, such as T waves.

Sensing circuitry also incorporates noise reversion circuits that cause the pacemaker to revert to a noise reversion mode (asynchronous pacing) whenever the rate of signal received by the sensing circuit exceeds the noise reversion rate. This feature is incorporated to prevent inhibition of pacing when the device is exposed to electromagnetic interference. Pulse generators also use Zener diodes designed to protect the circuitry from high external voltages, which may occur, for example, with defibrillation. When the input voltage presented to the pacemaker exceeds the Zener voltage, the excess voltage is shunted back through the leads to the myocardium.

The timing circuit of the pacemaker is a crystal oscillator that regulates the pacing cycle length, refractory periods, blanking periods and AV intervals with extreme accuracy. The output from the oscillator (as well as signals from the sensing circuitry) is sent to a timing and logic control board that operates the inter-

nal clocks, which in turn regulate all the various timing cycles of the pulse generator. The timing and logic control circuitry also contains an absolute maximal upper rate cut-off to prevent "runaway pacing" in the event of random component failure.<sup>55,56</sup>

Each new generation of pacemakers contains more microprocessor capability. The circuitry contains a combination of read-only memory (ROM) and random-access memory (RAM). ROM is used to operate the sensing and output functions of the device, and RAM is used in diagnostic functions. Larger RAM capability has allowed devices to store increased amounts of retrievable diagnostic information, with the potential to allow downloading of new features externally into an implanted device.

External telemetry is included in all implantable devices. The pulse generator can receive information from the programmer and send information back by radiofrequency signals. Each manufacturer's programmer and pulse generator operate on an exclusive radiofrequency, preventing the use of one manufacturer's programmer with a pacemaker from another manufacturer. Through telemetry, the programmer can retrieve both diagnostic information and real-time information on battery status, lead impedance, current, pulse amplitude and pulse duration. Real-time electrograms and marker channels can also be obtained with most devices. The device can also be directed to operate within certain limits and to store specific types of diagnostic information via the programmer.

The most recent change in telemetry is that of "remote" capability. Information exchange has traditionally occurred by placing and leaving the programming

'head' of the programmer over the pulse generator for the duration of the interrogation and programming changes. New telemetry designs allow the programming 'head' or 'wand' to be placed briefly over the pulse generator to establish identity of the specific model and pulse generator and then complete the bidirectional informational exchange at a distance, i.e. the 'wand' does not need to be kept in a position directly over the pulse generator. Finally, even the use of a wand for certain pulse generators is not required for remote programming.

### Pacemaker nomenclature

A lettered code to describe the basic function of pacing devices, initially developed by the American Heart Association and the American College of Cardiology, has since been modified and updated by the members of the North American Society of Pacing and Electrophysiology and the British Pacing and Electrophysiology Group (currently the Heart Rhythm Society).<sup>57</sup> This code has five positions to describe basic pacemaker function, although it obviously cannot incorporate all of the various special features available on modern devices (Table 1.1).

The first position describes the chamber or chambers in which electrical stimulation occurs. **A** reflects pacing in the atrium, **V** implies pacing in the ventricle, **D** signifies pacing in both the atrium and the ventricle, and **O** is used when the device has antitachycardia pacing (ATP) or cardioversion-defibrillation capability but no bradycardia pacing capability.

The second position describes the chamber or chambers in which sensing occurs. The letter code is

**Table 1.1** NBG\* code

<i>I</i>	<i>II</i>	<i>III</i>	<i>IV</i>	<i>V</i>
<i>Chamber(s) paced</i>	<i>Chamber(s) sensed</i>	<i>Response to sensing</i>	<i>Programmability, rate modulation</i>	<i>Multisite pacing</i>
O = None	O = None	O = None	O = None	O = None
A = Atrium	A = Atrium	T = Triggered	P = Simple programmable	A = Atrium
V = Ventricle	V = Ventricle	I = Inhibited	M = Multiprogrammable	V = Ventricle
D = Dual (A + V)	D = Dual (A + V)	D = dual (T + I)	C = Communicating	D = Dual (A + V)

\*The North American Society of Pacing and Electrophysiology and the British Pacing and Electrophysiology Group. Modified from Bernstein *et al.*<sup>57</sup> By permission of Futura Publishing Company.

the same as that in the first position, except that an **O** in this position represents lack of sensing in any chamber, i.e. fixed-rate pacing. (Manufacturers may use an **S** in both the first and the second positions to indicate single-chamber capability that can be used in either the atrium or the ventricle.)

The third position designates the mode of sensing, i.e. how the device responds to a sensed event. **I** indicates that the device inhibits output when an intrinsic event is sensed and starts a new timing interval. **T** implies that an output pulse is triggered in response to a sensed event. **D** indicates that the device is capable of dual modes of response (applicable only in dual-chamber systems).

The fourth position reflects both programmability and rate modulation. **O** indicates that none of the pacemaker settings can be changed by noninvasive programming, **P** suggests “simple” programmability (i.e. one or two variables can be modified), **M** indicates multiprogrammability (three or more variables can be modified) and **C** indicates that the device has telemetry capability and can communicate noninvasively with the programmer (which also implies multiprogrammability). Finally, an **R** in the fourth position designates rate-responsive capability. This means that the pacemaker has some type of sensor to modulate the heart rate independent of the intrinsic heart rate. All modern devices are multiprogrammable and have telemetry capability; therefore, the **R** to designate rate-responsive capability is the most commonly used currently.

The fifth position was originally used to identify antitachycardia treatment functions. However, this has been changed, and antitachycardia options are no longer included in the nomenclature. The fifth position now indicates whether multisite pacing is not present (**O**), or present in the atrium (**A**), ventricle (**V**) or both (**D**). Multisite pacing is defined for this purpose as stimulation sites in both atria, both ventricles, more than one stimulation site in any single chamber, or any combination of these.

All pacemaker functions (whether single- or dual-chamber) are based on timing cycles. Even the function of the most complex devices can be readily understood by applying the principles of pacemaker timing intervals. This understanding is critical to accurate interpretation of pacemaker electrocardiograms, especially during troubleshooting. Pacemaker timing cycles are described in detail in Chapter 7: Timing Cycles.

## Defibrillation basics

In 1899, Prevost and Battelli<sup>58</sup> noted that the “fibrillatory tremulations produced in the dog” could be arrested with the reestablishment of the normal heartbeat if one submitted the animal “to passages of current of high voltage.” Despite these early observations, decades elapsed before broad clinical applicability fueled interest in more widespread investigation of the mechanism underlying defibrillation. With the development of internal defibrillators in the late 1970s came a greater need to quantify defibrillation effectiveness, to understand the factors governing waveform and lead design, and to determine the effect of pharmacological agents on defibrillation. Remarkably, much of this work was done without a complete understanding of the fundamental mechanism of defibrillation.

This section reviews the emerging insights to the electrophysiological effects of shocks and how they are related to defibrillation. It also reviews the means of assessing the efficacy of defibrillation (the “defibrillation threshold”) and the important effects of waveform, lead design and placement, and pharmacological agents on defibrillation, with an emphasis on those principles pertaining to clinical practice.

## Electrophysiological effects of defibrillation shocks; antitachycardia pacing

Despite great strides made in understanding the technology required for defibrillation (e.g. lead design and position, waveform selection), the basic underlying mechanisms have not been definitively determined. A few contemporary theories accounting for how an electric shock terminates fibrillation coexist with some overlapping: critical mass, upper limit of vulnerability, progressive depolarization, and virtual electrode depolarization. These are discussed below in brief.

First, a brief review of the cardiac action potential will be useful to facilitate discussion of the effects of defibrillation. The surface electrocardiogram and intracardiac electrogram, common in clinical practice, are the result of extracellular potentials generated by myocardial action potential propagation. An action potential is the transmembrane voltage in a single myocyte over time (Fig. 1.17). The action potential upstroke (phase 0, or depolarization) is mediated by sodium ion flow through voltage-sensitive selective channels, and during ventricular activation it is registered on the sur-

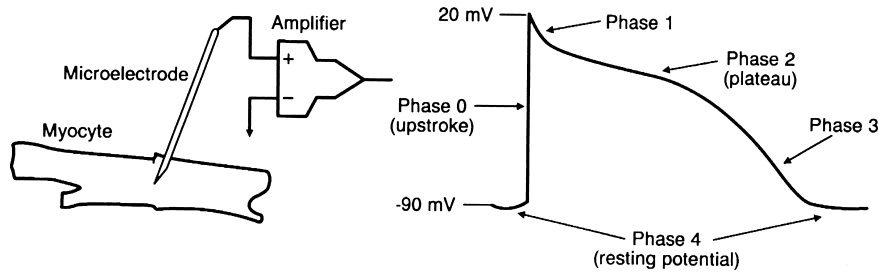


**Fig. 1.17** The cardiac action potential. Left, Impalement of a single myocyte by a microelectrode. This permits recording of the change in voltage potential over time in a single cell. Right, On the graph, voltage (in millivolts) is on the ordinate, time on the abscissa. The action potential in

ventricular myocytes begins with a rapid upstroke (phase 0), which is followed by transient early repolarization (phase 1), a plateau (phase 2), and terminal repolarization (phase 3), which returns the membrane potential back to the resting value.

face electrocardiogram as the QRS complex (Fig. 1.18). Repolarization (phase 3) of ventricular myocardium generates the surface electrocardiographic T wave. In its resting state, the myocardium is excitable, and a pacing stimulus, or current injected by the depolarization of a neighboring myocyte, can bring the membrane potential to a threshold value, above which a new action potential ensues. The ability of the action potential of a myocyte to depolarize adjacent myocardium results in propagation of electrical activity through cardiac tissue. Importantly, immediately after depolarization, the myocardium is refractory and cannot be stimulated to produce another action potential until it has recovered excitability (Fig. 1.19). The interval immediately after an action potential, during which another action potential cannot be elicited by a pacing stimulus, is referred to as the “refractory period.”

Ventricular fibrillation (VF) is the most common cause of sudden death. VF results when an electrical wavebreak induces re-entry and results in a cascade of new wavebreaks. In patients with a structurally abnormal or diseased heart, the underlying tissue hetero-

geneity results in a predisposition to wavebreak, then re-entry, and finally fibrillation.<sup>59</sup> These wandering wavelets are self-sustaining once initiated. In the 1940s, Gurvich and Yuniev<sup>60</sup> predicted that electric shocks led to premature tissue stimulation in advance of propagating wavefronts, preventing continued progression of the wavefront. This concept of defibrillation as a large-scale stimulation remains a central tenet of many of the currently held theories of defibrillation.

### Critical mass

The critical mass theory proposed that shocks need only eliminate fibrillatory wavelets in a critical amount of myocardium to extinguish the arrhythmia. Experiments in canine models found that injection of potassium chloride (which depolarizes myocardium, rendering it unavailable for fibrillation) into the right coronary artery or the left circumflex artery failed to terminate VF as often as injection into both the left circumflex and the left anterior descending arteries together. Similarly, electrical shocks of equal magnitude terminated fibrillation most frequently when the electrodes were

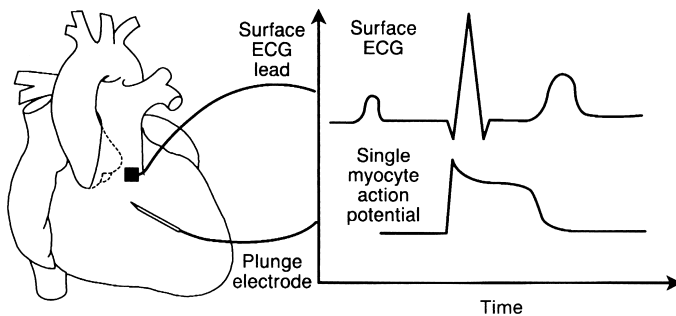


**Fig. 1.18** Correlation of cellular and clinical electrical activity. The QRS complex of the surface electrocardiogram (ECG) is generated by the action potential upstroke (phase 0) of ventricular myocytes and the propagation of the upstroke through the ventricular myocardium. Similarly, the T wave is the result of ventricular repolarization (phase 3).



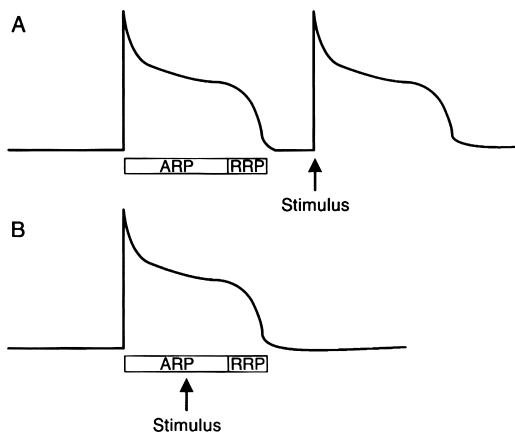


**Fig. 1.19** Refractory periods. Myocytes can be stimulated to generate new action potentials, except in their absolute refractory period (ARP). In (A), a stimulus occurs after the myocyte has fully recovered from the preceding action potential, and a new action potential ensues. In contrast, in (B), the same stimulus is delivered earlier, the myocyte remains in its absolute refractory period because of the preceding action potential, and no new action potential is elicited. RRP, relative refractory period.

positioned at the right ventricular apex and the posterior left ventricle, as opposed to two right ventricular electrodes. Thus, it was concluded that if a “critical mass” of myocardium was rendered unavailable for VF either by potassium injection or by defibrillatory shock, the remaining excitable tissue was insufficient to support the wandering wavelets, and the arrhythmia terminated.<sup>61</sup> However, it was not critical to depolarize every ventricular cell to terminate fibrillation.

#### Upper limit of vulnerability

Studies mapping electrical activation after failed shocks led to several observations not accounted for by the critical mass hypothesis, giving rise to the upper limit of vulnerability theory. First, an isoelectric interval (an electrical pause) was seen after failed shocks before resumption of fibrillation. The relatively long pause suggested that VF was terminated by the shock and then secondarily regenerated by it (Fig. 1.20).<sup>62</sup> The concept that failed shocks are unsuccessful because they give rise to a new focus of fibrillation rather than because they fail to halt continuing wavelets was further buttressed by a second observation—that postshock conduction patterns were not the continuation of preshock wavefronts.<sup>63</sup> If a failed shock resulted from the inability to

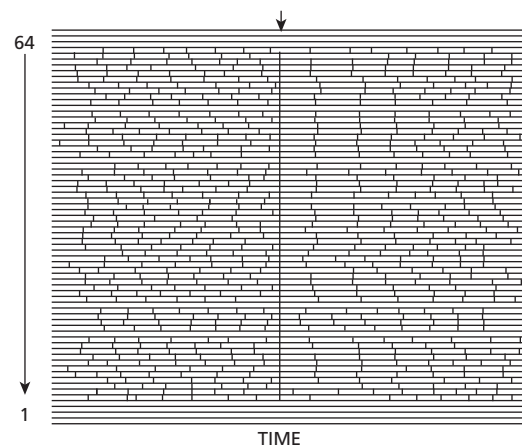


**Fig. 1.20** Isoelectric interval after failed shock. Tracings show recordings from 64 electrodes evenly distributed over the epicardial surfaces of both ventricles. At the arrow, an unsuccessful 1-J defibrillation shock is delivered. Note that an isoelectric interval (i.e. flat line without activations) immediately follows the shock, that temporal clustering of the first activation follows the failed shock, and that rapid degeneration back to fibrillation then occurs. (Modified from Chen *et al.*<sup>62</sup> By permission of American Society for Clinical Investigation.)

halt continuing fibrillation, the assumption was that the postshock wavefronts should be a continuation of the propagating wavefronts present before shock delivery and that new wavefronts at sites remote from the preshock wavefronts would not be expected. Furthermore, VF was frequently reinitiated in the regions of lowest shock intensity, suggesting that these low-intensity regions were responsible for reinitiating fibrillation.

Elegant mapping studies demonstrated that shocks with potential gradients less than a minimum critical value—termed the upper limit of vulnerability (ULV) (6V/cm for monophasic shocks, 4V/cm for biphasic shocks)—could induce fibrillation when applied to myocardium during its vulnerable period. Low-energy shocks did so by creating regions of functional block in vulnerable myocardium at “critical points” that initiated re-entry and subsequent fibrillation.<sup>64</sup> Figure 1.21 depicts the vulnerable zone during normal sinus rhythm. In sinus rhythm, low-energy shocks delivered during the T wave induce VF; higher energy shocks—with energy above the ULV—do not. Since at any given time during fibrillation a number of myocardial regions are repolarizing and thus vulnerable, a shock with a potential gradient below the ULV may create a

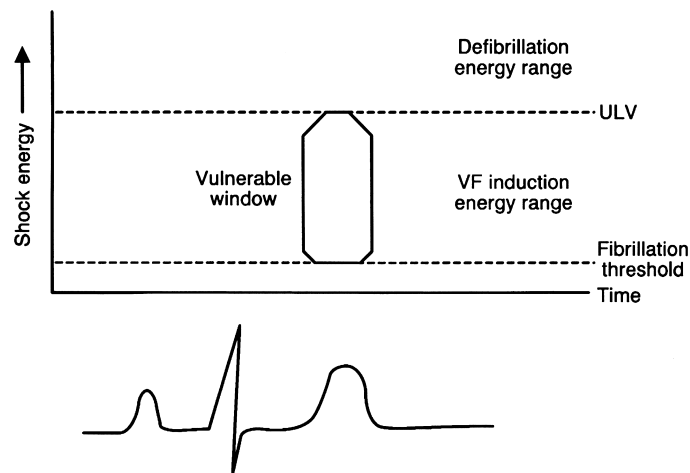


**Fig. 1.21** Window of vulnerability during sinus rhythm. During sinus rhythm, the ventricles are vulnerable to ventricular fibrillation (VF) when a shock is delivered on the T wave, in the vulnerable window. To induce fibrillation, the shock energy must be greater than the fibrillation threshold and below the upper limit of vulnerability (ULV). Shocks with energy above the upper limit of vulnerability do not induce fibrillation. Since during VF there is

dyssynchrony of activation, at any given instant a number of regions are repolarizing (equivalent to the T wave in sinus rhythm), so that a shock with a gradient that is less than the ULV can reinduce fibrillation in these regions. In contrast, shocks with energy above the ULV throughout the myocardium cannot reinitiate VF and are successful. The ULV is correlated with the defibrillation threshold. Further details appear in the text.

critical point and reinitiate fibrillation. Conversely, a shock with a gradient above the ULV across the entire myocardium does not reinduce VF and should therefore succeed. During defibrillator testing, shocks are intentionally delivered in the vulnerable zone to induce fibrillation (Fig. 1.22), and the zone of vulnerability has been defined in humans.<sup>65</sup> The fact that the vulnerable zone exists and that the ULV has been correlated with the defibrillation threshold supports the ULV hypothesis as a mechanism of defibrillation.<sup>66</sup>

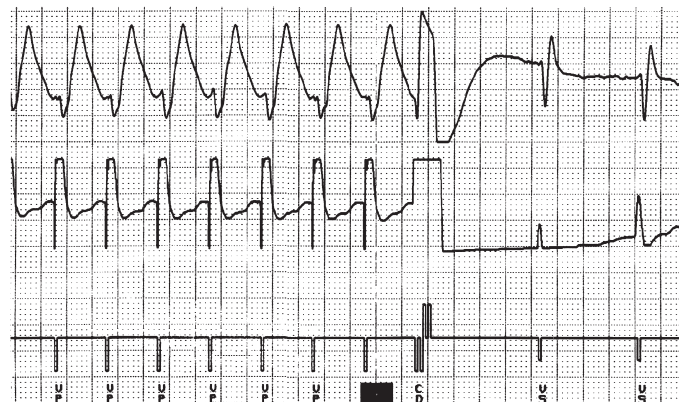
### Progressive depolarization

A third theory of defibrillation, the progressive depolarization theory (also referred to as the “refractory period extension theory”) incorporates some elements of both critical mass and ULV theories. Using voltage-sensitive optical dyes, Dillon and Kwaku<sup>67</sup> have demonstrated that shocks of sufficient strength were able to elicit active responses, even from supposedly refractory myocardium. Thus, as seen in Fig. 1.23A, the duration of an action potential can be prolonged (and the refractory period extended) despite refractory myocardium when a sufficiently strong shock is applied.<sup>68</sup> This phenomenon may result from sodium channel reactivation by the shock. The degree of ad-

ditional depolarization time is a function of both shock intensity and shock timing.<sup>69</sup> Since the shock stimulates new action potentials in myocardium that is late in repolarization and produces additional depolarization time when the myocardium is already depolarized, myocardial resynchronization occurs. This is manifested by myocardial repolarization at a constant time after the shock (second dashed line in Fig. 1.23, labeled “constant repolarization time”). Thus, the shock that defibrillates extends overall ventricular refractoriness, limiting the excitable tissue available for fibrillation. It thus extinguishes continuing wavelets and resynchronizes repolarization, so that distant regions of myocardium become excitable simultaneously, preventing dispersion of refractoriness and renewed re-entry. Experimental evidence has demonstrated that shocks with a potential gradient above the ULV result in time-dependent extension of the refractory period. In contrast, lower-energy shocks may result in a graded response that could create transient block and a critical point, thereby reinducing fibrillation.<sup>69</sup>

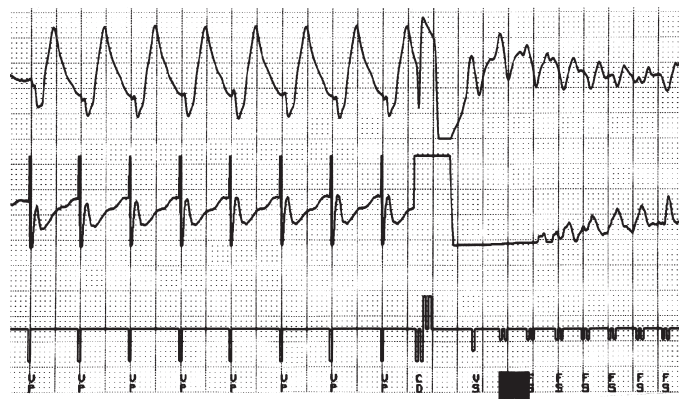
### Virtual electrode depolarization

More recently, optical signal measurements of trans-



A

**Fig. 1.22** Induction of ventricular fibrillation by a T-wave shock during testing of an implantable defibrillator. In (A), a 1-J shock is delivered 380 ms after the last paced beat. Fibrillation is not induced, because this shock is delivered outside the window of vulnerability. In (B), the timing of the shock is adjusted to 300 ms after the last paced complex, so that it is delivered more squarely on the T wave, in the window of vulnerability, and fibrillation is induced. The window of vulnerability is defined by both shock energy and timing. CD, charge delivered; FS, fibrillation sense; VP, ventricular pacing; VS, ventricular sensing.



B

membrane potentials have demonstrated the concept of the “virtual electrode.”<sup>70</sup> The virtual electrode effect makes the defibrillation electrode effectively much larger than the physical electrode. In the virtual electrode, the anode cells are brought close to their resting potential, increasing their responsiveness to stimulation. More importantly, the region of depolarization or hyperpolarization near the physical electrode is surrounded by regions with opposite polarity. Anodal shocking produces a wavefront which begins at the boundary of positively charged regions and then spreads in the direction of the negatively charged region of physical anode.<sup>71</sup> This produces “collapsing” wavefronts that frequently collide and neutralize one another and thereby are less likely to result in a sustained arrhythmia (Fig. 1.24).<sup>72</sup> This theory incorporates many aspects of the above-mentioned mechanisms.

To summarize and to put defibrillation theory into clinical perspective, the effects of the application of a voltage gradient across myocardium are a function

of field strength and timing. Although the biological effects of shocks may overlap, this concept is summarized in Fig. 1.25. Extremely low energy pulses may have no effect on the myocardium. Stronger pulses (in the microjoule range), such as those used for cardiac pacing, result in action potential generation in non-refractory myocardium, which leads to a propagating impulse. With increasing electric field strength (to the 1-J area), VF can be induced with shocks delivered during the vulnerable period. Increasing the shock strength above the ULV (and above the defibrillation threshold) puts the shock in the defibrillation zone. Very high-energy shocks can lead to toxic effects, including disruption of cell membranes, postshock block, mechanical dysfunction and new tachyarrhythmias.<sup>69</sup>

### Antitachycardia pacing

The concepts of basic myocardial function also explain the mechanism of arrhythmia termination with ATP.

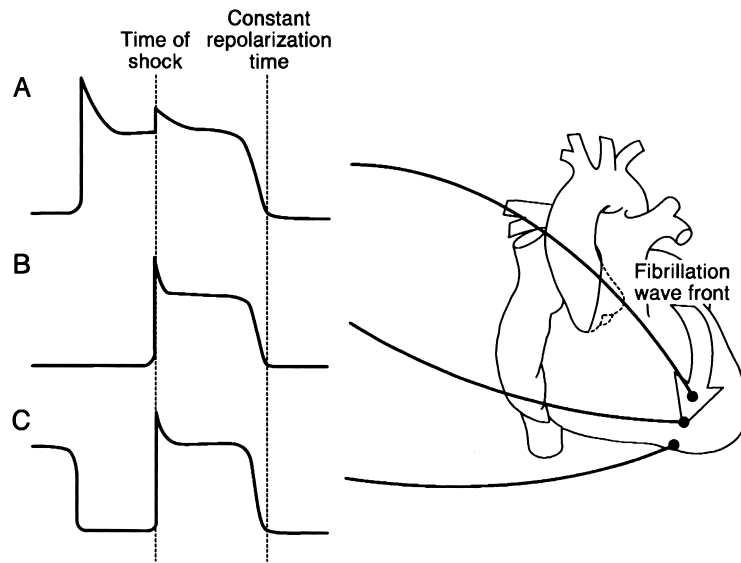


**Fig. 1.23** Progressive depolarization. A fibrillatory wavefront is depicted by the arrow, and the action potential response to a defibrillatory shock is demonstrated at several points surrounding the wavefront. The fibrillatory wavefront has just passed through a myocyte at point A when the shock is delivered. The myocyte is in its plateau (phase 2), when it would ordinarily be refractory to additional stimulation. However, when a sufficiently strong shock is delivered, the myocyte can generate an active response with prolongation of the action potential and of the refractory period. The response is referred to as “additional depolarization time.” The

tissue at point B is at the leading edge of the fibrillatory wavefront. The shock strikes this myocardium at the time of the upstroke (phase 0) and has little effect on the action potential. The tissue at point C is excitable (it is the excitable gap that the fibrillatory wave front was about to enter) when the shock is delivered. The shock elicits a new action potential in this excitable tissue. Despite the different temporal and anatomical locations of the three action potentials depicted, after the shock there is resynchronization by the “constant repolarization time.” This resynchronization helps prevent continuation of fibrillation.

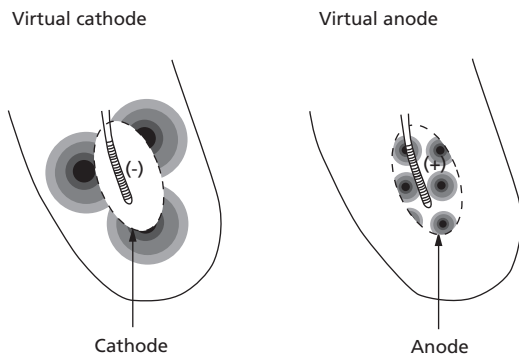


**Fig. 1.24** The cathodal shocks (left) produce wavefronts that expand and propagate away from the right ventricular coil. In comparison, anodal shocks (right) produced wavefronts that collapse and propagate towards the right ventricular coil (Adapted with permission from Figure 4, Kroll *et al.*<sup>70</sup> Present understanding of shock polarity for internal defibrillation: the obvious and non-obvious clinical implications).

As an example, in monomorphic ventricular tachycardia (VT) late after myocardial infarction, a re-entrant circuit utilizing abnormal tissue adjacent to an infarct is responsible for the arrhythmia (Fig. 1.26). For the re-entrant circuit to perpetuate itself, the tissue immediately in front of the leading edge of the wavefront must have recovered excitability so that it can be depolarized (Fig. 1.26). Thus, an excitable gap of tissue must be present in advance of the leading tachycardia wavefront or the arrhythmia will terminate. ATP—delivered as a short burst of pacing impulses at a rate slightly greater than the tachycardia rate—can terminate VT by depolarizing the tissue in the excitable gap, so that the tissue in front of the advancing VT wavefront becomes refractory, preventing further arrhythmia propagation (Fig. 1.26B). The ability of a train of impulses to travel to the site of the re-entrant circuit and interrupt VT depends on several factors,

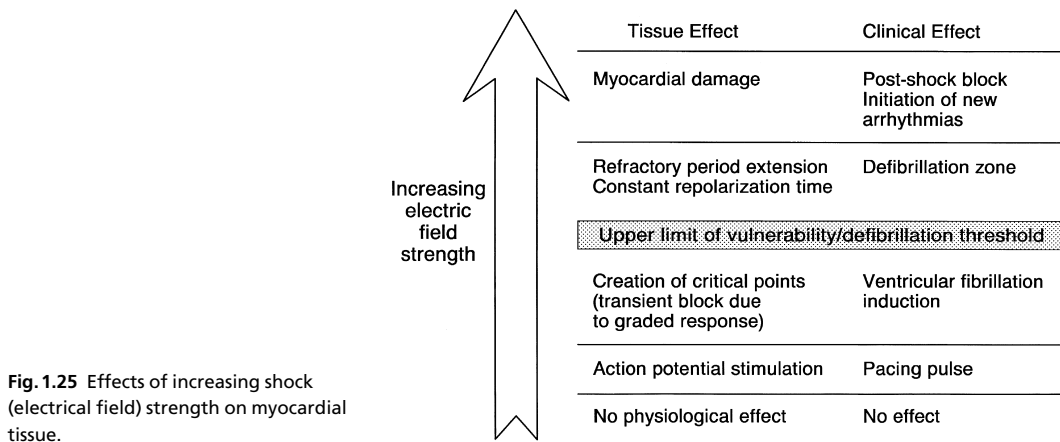


Fig. 1.25 Effects of increasing shock (electrical field) strength on myocardial tissue.

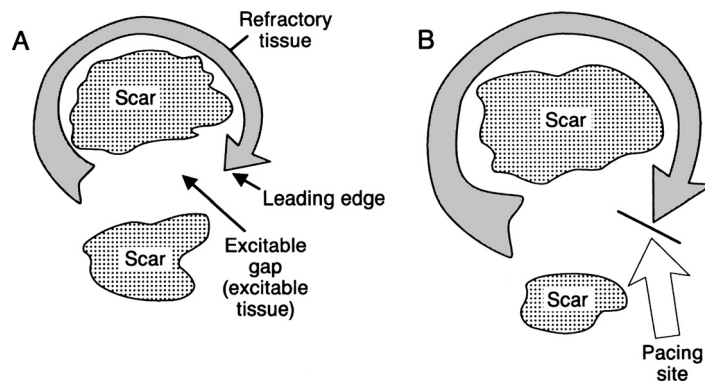


Fig. 1.26 Re-entrant ventricular tachycardia circuit. In (A), a circuit around a fixed scar is depicted by the arrow. The head of the arrow depicts the leading edge of the wavefront, and the body of the arrow back to the tail (colored gray) consists of tissue that is still refractory (since the wavefront has just propagated through it). The tissue between the tip and the tail of the arrow is excitable and is called the “excitable gap.” For the arrow head to continue its course around the

scar, an excitable gap must be present; if the wavefront encounters refractory tissue, it cannot proceed. In (B), a wavefront generated by an antitachycardia pacing impulse enters the excitable gap and terminates tachycardia. Tachycardias with a small excitable gap (i.e. the head of the arrow follows the tail very closely, so that only a small “moving rim” of excitable tissue is in the circuit) are more difficult to terminate with antitachycardia pacing.

including the site of pacing (the closer to the circuit entrance, the greater the likelihood of circuit penetration and termination), the length of the tachycardia cycle, and the size of the excitable gap. With delivery of ATP, faster and more remote circuits with smaller excitable gaps are generally more difficult to terminate and have a greater risk of degeneration to less organized tachyarrhythmias, including fibrillation.

To treat VT, ATP is delivered through a right ventricular lead in ICDs. ATP has been applied successfully to treat slow VT (<188–200bpm, success rate 78–91%)<sup>73</sup>, and recently fast VT (200–250bpm, success rate 72–81%)<sup>74</sup>. These therapy success rates are

reinforced by the observation that ATP did not result in an increased risk of acceleration of the arrhythmia, syncope, or mortality in comparison with patients who receive defibrillation shocks only.<sup>74</sup> Patients with ATP, rather than those programmed to defibrillation shocks only, also report statistically higher quality of life of scores. If ATP fails, or if the frequency of the VT is too high to apply ATP, the device diverts immediately to deliver a defibrillation shock. The use of ATP in the ventricle is important in limiting shocks, and is further discussed in Chapter 8. This chapter will also address the empiric use of ATP that may directly impact future appropriate shock therapies.

In addition to VT, atrial fibrillation and tachycardia occur frequently in patients with cardiac dysfunction, ventricular arrhythmias, and in patients with sinus node dysfunction.<sup>75-77</sup> ATP for atrial arrhythmias is also successful, with atrial tachycardia termination rates from 40 to 50%.<sup>78,79</sup> In addition to termination of the arrhythmia episode, ATP is also associated with an overall reduction in atrial tachycardia/atrial fibrillation burden.<sup>80</sup> Due to the absence of studies demonstrating clinically significant improvements with atrial ATP, its adoption in clinical practice has been modest. This may evolve with further studies.

The mechanisms underlying the success and failure of ATP are not fully understood. One theory is that ATP failure may occur when the pacing electrode is located too far from the re-entry core, and therefore unable to terminate the arrhythmia orthodromic wavefront.<sup>81</sup> However, this failure mechanism remains controversial. For example, a comparison of left vs. right ventricular ATP in induced VT showed both sites were equally effective, which raises questions regarding a location-dependent limitation.<sup>82</sup> Nevertheless, a recent study examined the potential therapy modification of biventricular antitachycardia pacing rather than right ventricular antitachycardia pacing to see if spatially distributed leads would advance the orthodromic wavefront and increase the likelihood of arrhythmia termination.<sup>83</sup> Although biventricular antitachycardia pacing was found to be superior in a rabbit model in terminating VT, there was also a theoretical increased risk of VT acceleration. This risk was not observed clinically in a study of patients who underwent cardiac resynchronization and ICD implantation, in which a significantly higher number of successful VT termination episodes were observed when biventricular ATP was used.<sup>84</sup> Next, the MIRACLE ICD trial showed that biventricular ATP improved VT termination, including those VTs that were classified as fast.<sup>85</sup> Finally, the ADVANCE CRT-D trial is an ongoing prospective trial that will examine the efficacy of right ventricular vs. biventricular ATP to terminate all types of VT.<sup>86</sup>

A promising new approach that is founded on the concepts of ATP is to deliver a low-voltage shock to “unpin” re-entry from its stationary core.<sup>81,87</sup> The method relies on the effect of virtual electrode polarization, which predicts hyperpolarization and depolarization on opposite sides of functional or anatomical heterogeneity that can result in secondary sources of excitation.<sup>81</sup> When a low voltage shock is properly timed,

all possible re-entry cores are simultaneously excited, which effectively destabilizes and unpins a re-entrant arrhythmia. In an experimental model using rabbits, the unpinning method terminated VT in all preparations, in comparison with 63% of preparations treated with standard ATP only. Although 35% of the preparations treated with unpinning first also required ATP, the study data suggested that this potential therapy was as effective as or potentially more effective than ATP for terminating stable, pinned re-entrant arrhythmias. Although promising, the role of unpinning in clinical practice is not yet established.

## Measuring the efficacy of defibrillation

### Threshold and dose–response curve

At the time of defibrillator insertion, it is important to determine whether the system implanted can successfully terminate fibrillation. A measure frequently used to assess the ability of a system to terminate VF is the defibrillation threshold (DFT). The term “threshold” suggests that there is a threshold energy above which defibrillation is uniformly successful and below which shocks fail (Fig. 1.27A). The multitude of factors that affect whether a shock will succeed—patient characteristics, fibrillation duration, degree of ischemia and potassium accumulation, distribution of electrical activation at the time of the shock, circulating pharmacological agents, and others—result in defibrillation behavior that is best modeled as a random variable, with a calculable probability of success for any given shock strength. Thus, defibrillation is more accurately described by a dose–response curve, with an increasing probability of success as the defibrillation energy increases (Fig. 1.27B). The curve can be characterized by its slope and intercept, and specific points on the curve can be identified, such as ED<sub>50</sub>, the energy dose with a 50% likelihood of success. Factors adversely affecting defibrillation shift the curve to the right, so that a higher dose of energy is required to achieve a 50% likelihood of success, and improvements in defibrillation (such as superior lead position and improved waveforms or lead design) shift the curve to the left (Fig. 1.28). Because of the large number of fibrillation episodes required to define a curve (30–40 inductions), the dose–response curve is not determined in clinical practice, but it remains a useful research tool and conceptual framework.

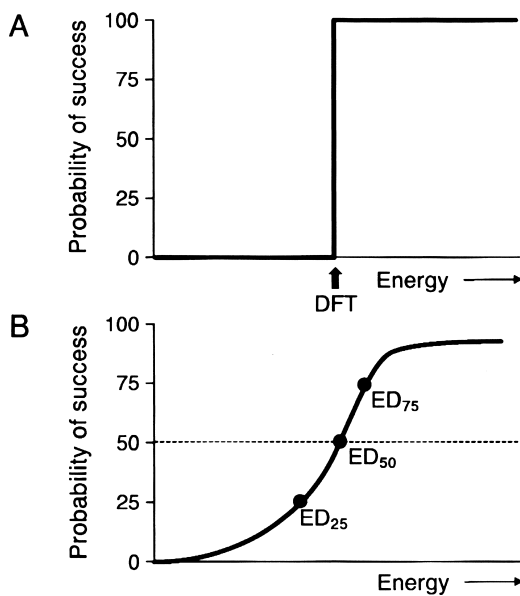


**Fig. 1.27** Defibrillation “threshold.” (A) The expected response to shock if a true threshold value existed. In reality, the likelihood of success is a sigmoidal dose–response curve, as shown in (B). The  $ED_{50}$  is the energy dose with a 50% likelihood of success, and so on.

### Relationship between defibrillation threshold and dose–response curve

If defibrillation is best described as a dose–response curve, where on the curve does the DFT exist (i.e. what is the probability of successful defibrillation at the clinically used DFT energy)? The probability of successful defibrillation at the DFT energy depends on the steps taken to define the threshold. Consider a step–down to failure DFT, in which shocks are delivered beginning at a relatively high energy (e.g. energy with a 99% success rate) and decremented by several joules with each VF induction until a shock fails (at which point a rescue shock is delivered). The DFT in this protocol is defined as the lowest energy shock that succeeds (Fig. 1.29). Since the initial energies tested are at the upper end of the dose–response curve, successive shocks may have a 98%, 95%, 88%, 85% (and so on) likelihood of success, depending on the starting energy and size of the steps taken. Despite the fairly high likelihood of success for each shock individually, the sheer number of shocks delivered in this range on average result in a shock failing (thus defining the DFT) at a relatively high point on the curve. If this process is repeated many times, a population of DFTs is created, with a mean and expected range. In humans, step–down to failure algorithms

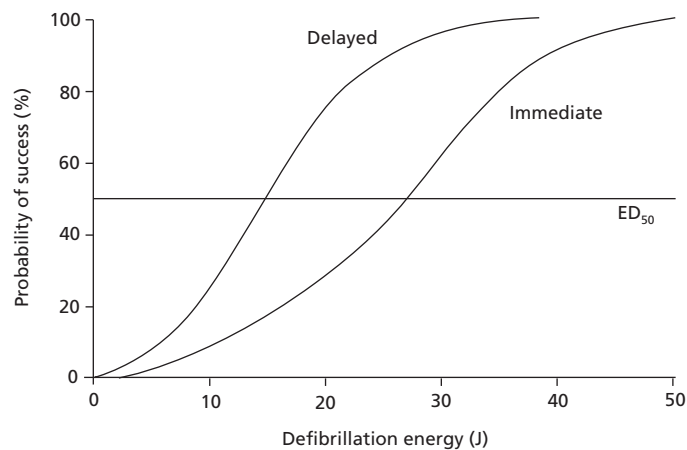


**Fig. 1.28** Use of dose–response curve to measure effects of an intervention on defibrillation efficacy. The graph shows the effect of thoracotomy on defibrillation in a canine model. The “immediate” group had defibrillation threshold testing done immediately after thoracotomy. Note that the curve is shifted to the right and that the energy with a 50% probability of success is 27 J, compared with 15 J for the “delayed” group, which was allowed 48–72 h of recovery before defibrillation testing.

Defibrillation is more effective in the “delayed” group because the probability of success at a given energy is higher in this group. Thus, the curves graphically display diminished defibrillation efficacy immediately after thoracotomy. (From Friedman PA, Stanton MS. Thoracotomy elevates the defibrillation threshold and modifies the defibrillation dose–response curve. *J Cardiovasc Electrophysiol* 1997; 8:68–73. By permission of Futura Publishing Company.)

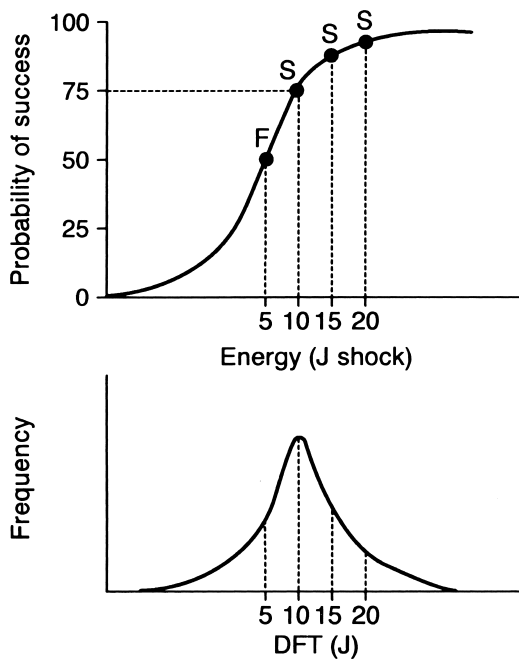


**Fig. 1.29** Step-down to failure defibrillation threshold (DFT) testing. In this hypothetical example (A), four shocks are required to define the DFT. The first shock is delivered at 20 J and is successful (S). The next shock, delivered at 15 J, also succeeds. A 10-J shock succeeds, and a 5-J shock fails (F), defining the DFT as 10 J (the lowest successful energy). Note from the curve that the likelihood of success at the DFT energy (10 J) is 70%. Now, if the DFT process were repeated, it is possible that the second shock might fail on one occasion (defining the DFT as 20 J) or that all four shocks might succeed on another occasion (and that a lower energy shock would fail to define the DFT), and so on. Thus, repeating the DFT determinations may result in different values for the DFT with each determination. However, if enough repetitions were performed, a population of DFTs, as shown in (B), would be created. The most commonly observed DFT in this example would be 10 J, which has a 70% likelihood of success. Further details in text.

have a mean DFT with likelihood of success near 70%, but with a standard deviation near 25%.<sup>88,89</sup> Thus, the likelihood of success of a shock delivered at the energy defined as the DFT at a single determination ranges from 25% to 88%, with an average of 71%.<sup>89</sup> In other words, if a defibrillator is programmed to the step-down to failure DFT energy for its first shock, the likelihood that that first shock will succeed can range from 25% to 88%, but on average will be 71%.

In contrast to the step-down to failure DFT, in a step-up to success DFT, low-energy shocks are deliv-

ered during VF with incremental doses of energy until a first success occurs, which defines the DFT. In this case, despite the fairly low likelihood of success at each low-energy shock, if enough shocks are delivered, one is likely to succeed, defining the DFT. With this protocol, the mean DFT has a likelihood of success near 30%. Iterative increment–decrement DFT or binary search algorithms that begin in the middle zone of the curve have been shown to approximate the  $ED_{50}$ , the energy with a 50% probability of success. In this type of protocol, if the first shock defibrillates the heart, the first shock of the next fibrillation episode uses a lower energy. If the first shock does not defibrillate the heart, a second shock at a higher energy is delivered.

Regardless of the DFT protocol, a DFT determination is best conceptualized as a means of approximating a point on the dose–response curve, with the specific point estimated being a function of the DFT algorithm chosen. DFT determinations can be very useful tools for assessing defibrillation efficacy. Triplicate DFT measurements, which can be performed with fewer than 10 fibrillation episodes, have been demonstrated to be as reproducible as the true logistic regression model of the dose–response curve and to have less variability than other models used to estimate dose–response curves. Thus, determination of a DFT before and after an intervention (such as initiation of a drug or movement of a lead to a new position) can determine whether defibrillation efficacy is enhanced or impaired by the intervention.

### Defining an implantation safety margin

Given that a DFT determination is an estimated point on the dose–response curve and that the probability of successful defibrillation at the DFT is approximately 70% with the commonly used step-down protocol, a safety margin must be added to the DFT energy to increase the odds of success. Although all device shocks could be programmed to deliver the maximum available energy, using a lower energy that can consistently terminate fibrillation has advantages. These include faster charge time and more prompt delivery of therapy (with reduced chance of syncope), battery preservation, diminished risk of AV block, decreased myocardial damage in the regions with the highest voltage gradient, and diminished risk of impaired postshock sensing.<sup>90,91</sup> These benefits must be weighed against the morbidity accrued by the requirement of a second shock and consequences of an extended



period of ventricular tachyarrhythmia. Thus, the energy programmed should be a value high enough above the DFT to ensure that the shock is on the “plateau” of the dose–response curve, where success rates exceed 90%, but not necessarily at maximum output. In humans, adding 10 J to the DFT has been shown to result in first-shock success rates of  $99.5 \pm 4.3\%$ .<sup>92,93</sup> If one shock fails, two of three successful shocks at a 10-J safety margin have been shown to predict an annual rate of sudden death of  $< 1\%$ .<sup>94</sup> Strategies using one defibrillation shock, or using no VF inductions, are emerging and increasingly used in practice, and discussed below.

### Defibrillation testing at implantation

With the information known about the human defibrillation dose–response curve and defibrillation models, a practical approach to implantation testing can be used. Step-down to failure DFT testing can be done with three or four episodes of fibrillation. However, given the high likelihood of successful implant with modern active can, biphasic, implantable systems, strategies using fewer shocks to assess the safety margin are increasingly popular. In our practice, we typically employ an approach that requires two VF inductions (discussed below).

For step-down to failure testing, external defibrillation pads are placed before the surgical implantation procedure begins. Testing is done with the device in the surgical pocket and with leads connected. The high-voltage lead impedances are measured to insure appropriate lead connections. Standard ICDs can deliver programmable energies up to 30–35 J. Higher-energy devices, with outputs as high as 40 J, are also available. The first-shock energy is programmed to 10 J less than the maximum output of the device, and fibrillation is induced. If the test shock is successful, the first-shock energy is lowered by 5 or 6 J, and after a delay of 3–5 min fibrillation is induced again and the new energy tested. This iterative decremental process is continued until the first shock fails or until an energy of 5 or 6 J succeeds (at which point the DFT is often defined as  $\leq 5$  or 6 J). The lowest successful energy is taken as the DFT, and the first shock of the device is chronically programmed to the DFT energy plus 10 J. Often during testing, the second defibrillator shock is programmed to an energy equal to the last successful shock energy plus 10 J, and rescue is performed by the defibrillator (rather than externally). Thus, after a 15-J shock is suc-

cessful, the first shock is programmed to 10 J for the next induction, and the second device shock is programmed to 25 J [which is the current lower boundary for the DFT (15 J) plus a 10-J safety margin].

Although step-down to failure testing is still occasionally used in our practice, we more commonly employ a technique utilizing two VF inductions. The first shock is set to 10 J less than the maximum device output. If successful, rather than stepping down by 5–6 J, for the second induction the first shock is programmed to 14 or 15 J, and the second shock is programmed to the same as the first shock. If the first shock succeeded, the approximate “DFT” is said to be  $\leq 15$  J, and if the second shock succeeds, the DFT is defined as that energy (typically 25 J). In our experience, patients with an active can, pectoral, biphasic DFT  $< 15$  J have a very low risk of subsequent inadequate defibrillation, and no additional testing is preformed until the time of pulse generator change out.<sup>95</sup> In patients in whom the DFT approximation is higher, additional testing may be done at implant or, more commonly, annually until a chronically stable DFT is confirmed. Two successes at an energy 10 J less than the maximum device output are required to achieve a 10-J safety margin. If these are not achieved, system modification is required, as discussed below.

Some experts recommend a second strategy that emerged from the low energy safety study (LESS) trial.<sup>96</sup> In a substudy of the LESS trial, Higgins *et al.*<sup>97</sup> reported that a single conversion success at 14 J on the first ventricular induction yielded a similar positive predictive accuracy (91%) as the commonly accepted approach of two successes at 17 J or 21 J in determining a successful outcome with a device that provided 31 J. However, an approach that utilized successes at 21 J provided the highest combination of positive and negative predictive accuracy (98.8% and 100%, respectively). Nonetheless, a subset analysis by Gold *et al.*<sup>98</sup> showed that the results were durable, in that those patients in whom the VF induction test was successful with a first 14-J shock at implantation, regardless of additional induction tests, had similar long-term VF conversion success rates as all ICD recipients when the device was programmed to provide 31 J.

If an adequate safety margin is not demonstrated, a common next step is to reverse the shock polarity (waveform and polarity are discussed in greater detail below). In Table 1.2, potential options are provided if

---

Reverse the shock polarity
Change shock configuration (example tip-to-generator, ring-to-generator, tip-to-coil)
Waveform modification if available with the generator
Exchange the generator to a "high-output" device
Exclude if possible drugs that increase the defibrillation threshold
Add a superior vena cava coil
Add a subcutaneous array or patch
Move the generator to a left pectoral position if located on the right

---

**Table 1.2** Options in a patient with high energy requirements or an inadequate safety margin at defibrillation threshold testing.

an adequate safety margin is not demonstrated. Currently available devices also allow the programming of multiple potential configurations to alter the shock vector [e.g. exclusion of the superior vena cava coil, or of the can (particularly if it is placed in the right chest), etc.]. If implantation criteria are still not met, some devices permit waveform pulse width adjustment (discussed below). Alternatively, a high-output device is used, leads are repositioned if it is thought that lead position can be improved, or an additional endovascular lead is added in systems that permit it. If these approaches fail, a subcutaneous lead is added (see Chapter 5 for implantation technique). Using biphasic waveforms, we have found that subcutaneous leads are required in only 3.7% of devices implanted.<sup>99</sup>

In a single-center observational study of three types of subcutaneous leads (single-element subcutaneous array electrode, three-finger electrodes, subcutaneous patch electrodes), all types performed well without a significant change in defibrillation threshold observed.<sup>100</sup> Although there was no significant difference in complications, 7.3–9.5% of patients developed a major complication (predominantly lead fracture). Therefore, with use of a subcutaneous ICD lead, patients require close follow-up with routine chest radiographs.

There are many factors that may result in elevated defibrillation threshold. These include drug therapy, underlying cardiac disease, the size, configuration and number of defibrillating leads, the time that VF persists before shock delivery, ischemia, hypoxia, amplitude of the VF waveform, temperature, heart weight, body weight, direction of the delivered shock and waveform, and chronicity of lead implantation.<sup>101</sup> In patients with inherited channelopathies, such as Brugada syndrome, high defibrillation thresholds may be

prevalent and problematic.<sup>102</sup> In one series of patients who received a high-output generator for an elevated defibrillation threshold, the majority had underlying coronary artery disease, with reduced left ventricular function, and were on amiodarone.<sup>101</sup> An important finding in this study was that in patients with high defibrillation thresholds who receive an ICD, arrhythmia death remained a significant long-term risk (42% of the deaths were arrhythmia related).

An interesting observation is that there is a circadian variation in the defibrillation threshold. The defibrillation threshold has a morning peak that is 16% higher than that measured after noon.<sup>103</sup> In addition, the first failed shock rate is more often in the morning compared with other times during the day. This variability in defibrillation threshold is clinically important in patients with high thresholds, in whom a 10-J safety margin becomes more difficult to achieve.

Finally, with the advent of newer ICD technologies that utilize different waveforms and allow various shock configurations, some investigators have begun to ask whether DFT testing is required. In general the likelihood of a high DFT is low. However, in one contemporary observation study >6% of patients required modification of their ICD system due to an inadequate safety margin.<sup>104</sup> In some patients DFT testing is postponed due to other comorbid illness, such as an individual with atrial fibrillation and not on anticoagulation. These patients may account for up to 5% of patients who undergo ICD implantation. In considering the decision to perform DFT testing, other potential benefits of the study must be considered. For example, DFT testing may identify lead dysfunction, demonstrates appropriate sensing and charging of the device, and in general test the complete system integrity.<sup>105</sup> These benefits must be

**Table 1.3** Contraindications to ICD implant testing<sup>106</sup> (Reproduced with permission from Blackwell Publishing.)

---

*Absolute contraindication*

Risk of thromboembolism  
 Left atrial thrombus  
 Left-ventricular thrombus, not organized  
 Atrial fibrillation in the absence of anticoagulation  
 Inadequate anesthesia or anesthesia support  
 Known inadequate external defibrillation  
 Severe aortic stenosis  
 Critical, non-revascularized coronary artery disease with jeopardized myocardium  
 Hemodynamic instability requiring inotropic support

---

*Relative contraindication*

Left ventricular mural thrombus with adequate systemic anticoagulation  
 Questionable external defibrillation (e.g. massive obesity)  
 Severe unrevascularized coronary artery disease  
 Recent coronary stent  
 Hemodynamic instability  
 Recent stroke or transient ischemic attack  
 Questionable stability of coronary venous lead

---

weighed against the risks of the procedure. Contraindications to ICD implant testing have been published, and are listed in Table 1.3.<sup>106</sup>

### Upper limit of vulnerability to assess safety margin

As previously discussed, the ULV is the lowest energy above which shocks delivered during the vulnerable period do not induce fibrillation. Numerous studies have demonstrated that the DFT and ULV are strongly linked.<sup>107-110</sup> Since the DFT and ULV are correlated, some investigators have suggested that ULV determinations could be performed to assess defibrillation efficacy with one or no fibrillation episode.<sup>107</sup> During sinus rhythm, test shocks are delivered at the peak of the T wave at initially high energies, with the energy level subsequently decreased in steps until fibrillation is induced, defining a shock that is below the ULV. Since the ULV may be dependent on the coupling interval, energies are also delivered at various intervals before the T-wave peak to “scan” repolarization. For conventional biphasic waveforms, the ULV corresponds to a 90% successful energy level, and it has been used to provide adequate safety margins at cardioverter defibrillator implantations and for long-term follow-up in clinical protocols.<sup>111,112</sup> However, since ULV assessment is an indirect measure of defibrillation efficacy, the relationship between the ULV and the DFT may be affected by

numerous factors, including electrode configuration, pharmacological agents, and the protocol used to determine the ULV. Important in the patient population that receive an ICD, acute ischemia may reduce the ULV. This phenomenon is felt to be due in part to conduction failure during acute ischemia.<sup>113</sup> In some situations, the changes in ULV may not accurately reflect defibrillation efficacy. Since ULV may result in device testing with no VF induction, the R wave should be  $\geq 7$  mV to insure adequate sensing of VF. In the small subset of patients with ULV > 20 J, some experts advocate performing DFT testing at implant.<sup>114</sup> Because of the indirect nature of the ULV–DFT relationship and the large body of clinical and experimental data based on DFTs, ULV testing has only been adopted as routine clinical practice in a few centers. If future ICDs adopt automatic ULV testing (in which the device would scan the T wave and determine appropriate shock timing), this technique may become more widespread due to its ability to assess defibrillation efficacy without VF inductions in many patients and the possibility of automated testing by the ICD.

### The importance of waveform

The shape of a defibrillating waveform can dramatically affect its defibrillation efficacy. In the canine model, for example, Schuder *et al.*<sup>115</sup> demonstrated that for trans-

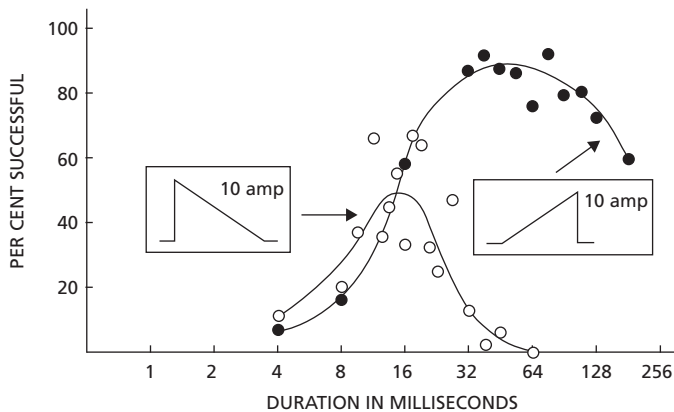


**Fig. 1.30** Effect of waveform on defibrillation. The ordinate shows the percentage of successful transthoracic canine defibrillation; on the abscissa is the duration of 10-A triangular shock. The success rate is greater for the ascending ramp than it is for the descending ramp. (From Schuder JC, Rahmoeller GA, Stoeckle H. Transthoracic ventricular defibrillation with triangular and trapezoidal waveforms. *Circ Res* 1996; 19:689–94. By permission of the American Heart Association.)

thoracic defibrillation, an ascending ramp waveform has a much higher success rate with the same delivered current than does a descending ramp (Fig. 1.30). This has been confirmed in a human study of 63 patients in which a 7-ms ascending ramp waveform significantly reduced delivered energy (18%) and voltage (24%) at DFT.<sup>116</sup> However, because of the importance of using physically small circuits for implantable devices, a capacitor discharge, which more closely resembles the descending ramp is employed in devices.

### Creating the defibrillation waveform

As in pacing, the battery serves as the source of electrical charge for cardiac stimulation in defibrillation. Before a high-energy shock can be delivered, the electrical charge must be accumulated in a capacitor, because a battery cannot deliver the amount of required charge in the short time of a defibrillation shock. A capacitor stores charge by means of two large surface area conductors separated by a dielectric (poorly conducting) material, and capacitor size is an important determinant of implantable defibrillator volume, typically accounting for approximately 30% of device size. If fluid analogies are used for electricity—voltage as water pressure and current as water flow (i.e. liters per minute)—the capacitor is analogous to a water balloon, which has a compliance defined by the ratio of volume to pressure. To increase the amount of water put into the balloon, one can increase the pressure or, alternatively, use a balloon with a greater compliance (more stretch for a given amount of pressure). Similarly, the charge stored can be increased by increasing capacitance or by applying greater voltage. The trend

in implantable devices has been toward smaller capacitors to create smaller devices.

The charge stored by a capacitor is defined by

$$\text{Charge} = \text{capacitance} \times \text{voltage}$$

The voltage waveform of a capacitor discharged into a fixed-resistance load (Fig. 1.31A) is determined by

$$V(t) = V_i \cdot e^{-t/RC}$$

and the energy associated with the waveform is given by

$$\text{Energy} = 0.5 CV^2$$

Since the “tail” of the waveform in longer pulses ( $\geq 10$  ms) rebrillates the ventricle (most likely accounting for the superiority of the ascending ramp seen by Schuder *et al.*<sup>115</sup>), truncated waveforms have been used clinically. The classic monophasic truncated waveform is shown in Fig. 1.31B. The waveform is characterized by the initial voltage ( $V_i$ ), the final voltage ( $V_f$ ), and the pulse width or tilt. Tilt is an expression of the percentage decay of the initial voltage. The tilt of a waveform is a function of the size of the capacitor used, the resistance of the leads and tissues through which current passes, and the duration of the pulse. Tilt is defined by the percentage decrease of the initial voltage:

$$\text{Tilt} = (V_i - V_f) / V_i \times 100\%$$

As shown in Fig. 1.31, tilt can have an important effect on defibrillation efficacy, with progressive improve-

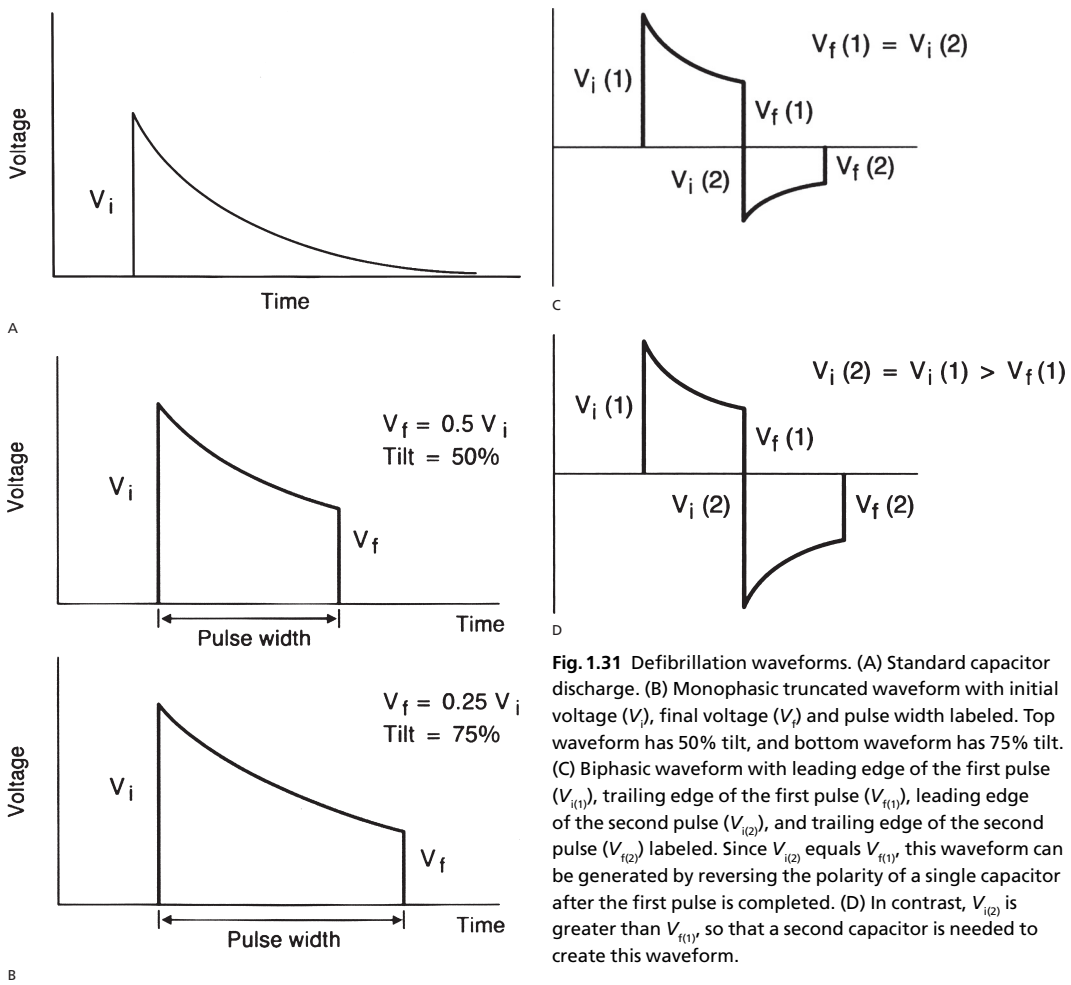


**Fig. 1.31** Defibrillation waveforms. (A) Standard capacitor discharge. (B) Monophasic truncated waveform with initial voltage ( $V_i$ ), final voltage ( $V_f$ ) and pulse width labeled. Top waveform has 50% tilt, and bottom waveform has 75% tilt. (C) Biphasic waveform with leading edge of the first pulse ( $V_{i(1)}$ ), trailing edge of the first pulse ( $V_{f(1)}$ ), leading edge of the second pulse ( $V_{i(2)}$ ), and trailing edge of the second pulse ( $V_{f(2)}$ ) labeled. Since  $V_{i(2)}$  equals  $V_{f(1)}$ , this waveform can be generated by reversing the polarity of a single capacitor after the first pulse is completed. (D) In contrast,  $V_{i(2)}$  is greater than  $V_{f(1)}$ , so that a second capacitor is needed to create this waveform.

ment in defibrillation efficacy with decreasing tilt, for a trapezoidal waveform of constant duration. For monophasic waveforms formerly used clinically, the optimal tilt was 50–80%.

**Biphasic waveforms**

Appropriately characterized biphasic shocks can result in significant improvement in defibrillation efficacy, with reductions in DFTs of 30–50%.<sup>117</sup> All currently available commercial defibrillators use biphasic waveforms; a typical biphasic waveform is shown in Fig. 1.31C. Biphasic waveforms have numerous clinical advantages, all stemming from their improved defibrillation efficacy. Biphasic waveforms have been shown to result in higher implantation success rates due to their lower DFTs, which are associated with higher safety margins.<sup>118</sup> Since safety margins are

increased, most patients do not require high-energy shocks, and smaller devices can be designed.<sup>119</sup> The improved efficacy of biphasic waveforms permits a greater tolerance in electrode positioning than that required for monophasic waveforms, facilitating the implanting procedure. Additionally, biphasic shocks have been shown to result in faster postshock recurrence of sinus rhythm and to have greater efficacy than monophasic shocks at terminating VF of long duration.<sup>120,121</sup>

With the development of biphasic defibrillation waveforms the energy required for defibrillation has been reduced.<sup>116,122,123</sup> Simultaneously, advances in capacitor and battery technology have allowed for a reduction of pulse generator size. Further advances that will reduce the generator size will occur when the energy required for defibrillation is reduced.<sup>116</sup>

### Phase duration and tilt

In most commercially available ICDs, pulse duration and tilt are pre-set to values found to be optimal based on experimental evidence (Figs 1.32 and 1.33). Some devices do permit individualization of the pulse widths, based on the concept that individual

variations in cellular time constants result in varying optimal pulse durations. Anecdotal observations and small studies support pulse width optimization in high DFT patients.<sup>124,125</sup> With few studies that specifically address this concept, individualized variation for optimization in patients with a high DFT requires further study.

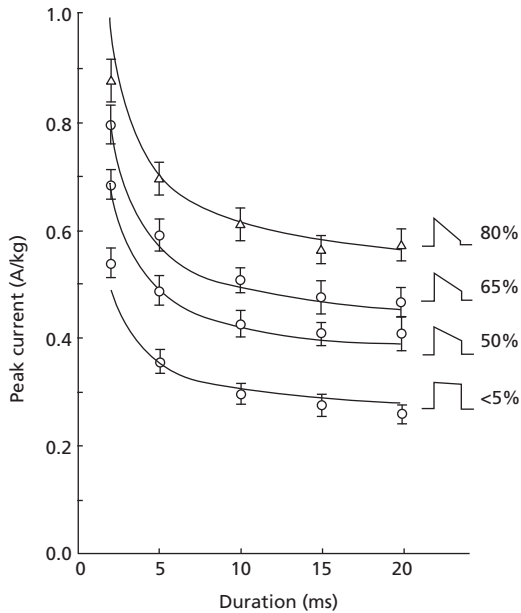


**Fig. 1.32** Internal canine defibrillation threshold (peak current) plotted against waveform duration and tilt. Note important effect of tilt on threshold with this waveform. (From Wessale JL, Bourland JD, Tacker WA, Geddes LA. Bipolar catheter defibrillation in dogs using trapezoidal waveforms of various tilts. *J Electrocardiol* 1980; 13:359–65. By permission of Churchill Livingstone.)

### Polarity and biphasic waveforms

Polarity is an important determinant of monophasic defibrillation, with lower DFTs found for transvenous systems when the right ventricular electrode is the anode (+).<sup>126,127</sup> The results of studies of biphasic polarity are less uniform, with some reports showing an effect of biphasic polarity and others indicating no effect.<sup>128,129</sup> However, all studies demonstrating a polarity effect have found that waveforms with a first phase in which the right ventricular electrode is the anode (+) are more effective. Additionally, biphasic polarity has the greatest effect on patients with elevated DFTs. In a study of 60 patients, use of biphasic waveforms with a right ventricular anodal first phase resulted in a 31% reduction in DFT in patients with DFT  $\geq 15$  J, whereas polarity made no difference in patients with DFTs  $< 15$  J.<sup>130</sup> Despite the fairly uniform population improvement in DFT with a ventricular anodal first phase polarity among studies in which an effect was seen, there is clearly individual variability, so that if an adequate safety margin cannot be found in a patient, a trial of the opposite polarity is reasonable, regardless of the initial polarity tested.

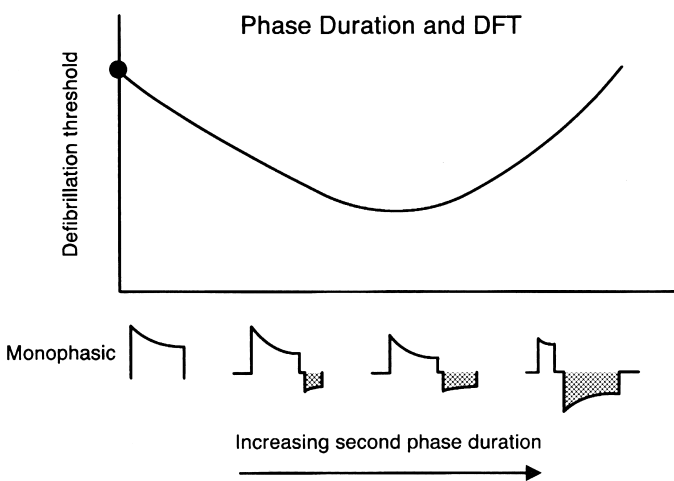


**Fig. 1.33** Idealized curve demonstrating the relationship between second phase duration and defibrillation threshold (DFT). Details are in the text. (From Wessale JL, Bourland JD, Tacker WA, Geddes LA. Bipolar catheter defibrillation in dogs using trapezoidal waveforms of various tilts. *J Electrocardiol* 1980; 13:359–65. By permission of Churchill Livingstone.)

### Mechanism of improved efficacy with biphasic waveforms

Several theories have been proposed to explain the observed superiority of biphasic over monophasic waveforms. None provides a complete explanation for the benefits seen, and the fundamental mechanism remains to be determined. However, important basic observations have been made.

#### Ascending ramp waveform

Mathematical models that predict defibrillation efficacy suggest that use of an ascending ramp waveform may improve efficacy of defibrillation. The waveform uses an ascending ramp phase over a predetermined time interval in the first phase.<sup>116,131-133</sup> In animal models, ascending ramp waveforms were more effective than truncated exponential waveforms.<sup>134</sup> In a recent randomized trial, patients were divided into two groups, one with a 12-ms ascending first phase and the other with a 7-ms ascending first phase. In those patients randomized to the 7-ms ascending first phase, the energy and voltage required at DFT were significantly reduced in comparison with the other group.<sup>116</sup>

#### First phase as “conditioning” pulse

Successful defibrillation requires sodium channel activation at a time when cells are ordinarily not receptive to physiological stimulation. The first phase of a pulse may serve to hyperpolarize tissue near the anode, thereby reactivating otherwise inactive sodium channels. This conditioning pulse facilitates excitation by the following pulse.<sup>135</sup>

#### Refractory period shortening

The first phase of a biphasic pulse may shorten the refractory period of myocardial cells. This transient shortening may then facilitate the effective recruitment of sodium channels by the second phase of the pulse. This ultimately extends the duration of the action potential and the refractory period, important putative mechanisms for defibrillation.<sup>136</sup>

#### Membrane stabilization

In addition to being more effective and requiring a lower potential gradient for defibrillation, biphasic waveforms are less toxic than monophasic waveforms. In higher voltage gradient regions, membrane disruption and myocardial damage may result from the shock. However, higher voltage gradients are required

to produce these toxic effects with biphasic waveforms than with monophasic waveforms. Deleterious postshock effects may be due to membrane microlesions, which permit indiscriminate exchange of ions. The reversal of polarity during the shock may expedite membrane reorientation and repair, decreasing postshock dysfunction.<sup>137</sup>

#### Measuring shock dose

All the discussion to this point has described the shock dose in terms of energy (joules). As noted above, the shape of the waveform is a function of the initial voltage, the size of the capacitor, and the resistance of the load. If a smaller capacitor is used to diminish device size, a larger initial voltage may be needed to deliver an equivalent amount of charge into the fibrillating tissue. Thus, two waveforms may have different leading edge voltages, but the same energy if there are differences in capacitance (Fig. 1.34). Therefore, the question of how to determine the “dose” of a shock arises. It is clearly important, because shocks of insufficient dose fail to terminate fibrillation and excessively strong shocks can lead to proarrhythmia or myocardial injury. The “dose” of defibrillation is usually given in units of energy (joules) on the basis of tradition and ease of measurement. Physiologically, however, energy has little bearing on defibrillation; the voltage gradient is the factor that affects membrane channel conductance, and at the tissue level several decades of animal and human research have shown current to be the most important factor for generating action potentials and for defibrillation.<sup>69</sup> To add to the complexity, energy

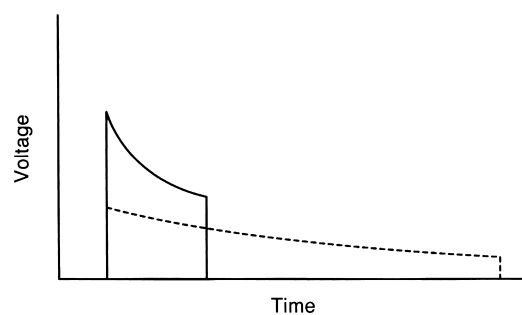


**Fig. 1.34** Two waveforms with different voltages but the same energy. The solid waveform has a higher initial voltage but a smaller capacitance and, consequently, a shorter pulse width. The dashed waveform starts with a lower voltage but has a greater capacitance and pulse width, resulting in the same energy delivery despite the marked differences in the voltages. Further details in the text.

can be described as the stored energy—the amount of energy stored in the capacitor before shock delivery—or the energy delivered. Since the waveforms are truncated, usually around 10% of the stored energy is not delivered. Additionally, although the term is used clinically, “delivered energy” is highly variable, depending on where the delivery is recorded; energy delivered at the lead surface is not the same as energy delivered only a few millimeters into the tissue. Some device manufacturers, in fact, simply report an arbitrary percentage of the stored energy as the delivered energy. Stored energy, although not a direct indicator of the factors responsible for biological defibrillation, indicates the size of the device necessary to generate a given energy shock. Over the range of clinically utilized capacitor size and biological tissue resistance in a given system, a change in energy up or down is reflected by a similar change in voltage and current. In practice, “energy” is the most commonly used term to indicate shock dose.

### Use of waveform theory in clinical practice

The optimal biphasic waveform is specific to the device, lead, and patient. In many commercially available devices, the only programmable option is the polarity. Therefore, if a patient undergoing implantable defibrillator insertion does not have an adequate defibrillation safety margin, a logical next step is reversal of polarity. If an adequate safety margin is still not met, a lead is often added (discussed below). Tilt or duration can also be modified as an alternative next step in systems that offer this feature.

### Lead system and defibrillation

The most efficient lead system is one that evenly distributes the shock over the myocardium and minimizes the difference in potential between high-gradient and low-gradient zones. This is best accomplished with large contoured epicardial patches positioned so that an imaginary line connecting the centers of the electrodes passes through the ventricular center of mass.<sup>138</sup> However, since epicardial leads require thoracotomy for placement, they are typically used after other approaches have been exhausted.

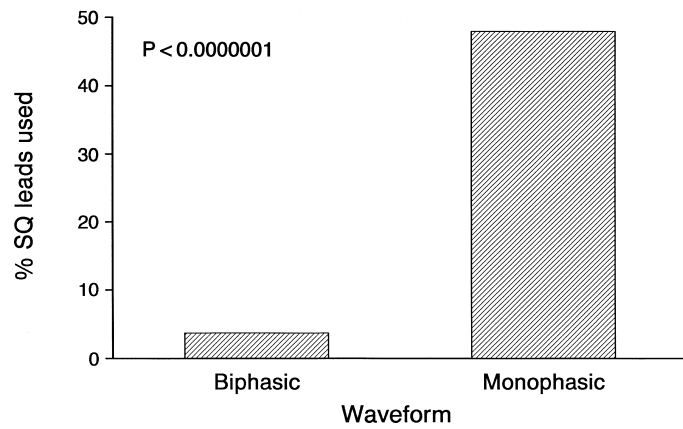
Although intrinsically less efficient, transvenous lead systems can now be used almost universally because of the adoption of biphasic waveforms (discussed above) and the introduction of defibrillators in

which the pulse generator shell is an active electrode. Because the surface area of the pulse generator is large, the addition of the generator shell as an active electrode reduces the biphasic endocardial DFT by 30% compared with that of a dual-coil defibrillation lead alone.<sup>139</sup> When an active can system with a single distal defibrillation coil is used, addition of a proximal coil has further lowered the DFT in some, but not all, studies.<sup>139,140</sup> Nevertheless, if implantation safety margins cannot be achieved despite waveform modification (reversal of polarity and, if available, adjustment of pulse width), adding a second lead with the electrode positioned near the junction of the right atrium and superior vena cava is a logical next step. Alternatively, since most leads in use today have two coils, in a subset of patients defibrillation is improved when the proximal coil is removed from the defibrillation circuit. This observation probably results from individual anatomical variations such that the proximal coil may lessen the field strength over the left ventricle. Anecdotally, use of three right ventricular coils (placement of a dual coil lead in the apex, and use of adapter to place a single coil lead in the outflow tract, with passage of shock from the two distal coils to the proximal coil and can) may help in high DFT situations, although this has not been validated. If adequate safety margins cannot be achieved despite optimal deployment of endovascular leads, subcutaneous patches or arrays, which further significantly increase defibrillation electrode surface area and can favorably direct greater current through the ventricles, can lead to successful implantation. With biphasic active-electrode pulse generators, the addition of subcutaneous leads is required in only 3.7% of patients (Fig. 1.35).<sup>99</sup> When they are required, arrays may be more effective than patches, though we found that this benefit was blunted in biphasic systems.<sup>99</sup>

As noted above, defibrillation efficacy is improved with optimal lead positions, although the effectiveness of biphasic waveforms, the large surface area of the pulse generator, and programmability that has allowed multiple potential vectors to be used that take advantage of the geometry of the leads and can, have permitted tolerance of less than perfect positions. Generally, defibrillation effectiveness diminishes as the right ventricular electrode is placed in a progressively proximal position, toward the tricuspid valve. Therefore, this lead should be placed as apically as possible. Additionally, a septal location, to direct as much of the electrical field over the left ventricular mass as possible, is desir-



**Fig. 1.35** Effect of waveform on frequency of subcutaneous (SQ) lead use. On the ordinate is the frequency of subcutaneous lead usage, and on the abscissa are the subgroups analyzed. In 45 of 94 (48%) patients with monophasic systems, subcutaneous leads were required to meet implantation criteria. In contrast, only 17 of 460 (3.7%) biphasic systems required subcutaneous leads to meet implantation criteria. (From Trusty *et al.*<sup>99</sup> By permission of Futura Publishing Company.)



able.<sup>141</sup> Active pulse generator shell permits independent positioning of a proximal defibrillation coil, and the proximal lead position can be near the superior vena cava, near its junction with the right atrium, or in the left subclavian vein (Fig. 1.36).<sup>142</sup>

Since in nearly all commercially available defibrillators the pulse generator shell serves as an electrode, its position can also affect defibrillation efficacy. Implantable defibrillators are most commonly placed in the left pectoral region, typically in the prepec-

toral (subcutaneous) plane. However, the site of pulse generator placement and vascular access is influenced by multiple factors, including patient and physician preference, anatomical anomalies, previous operations, integrity of the vascular system, and whether a preexisting permanent pacing system is present. In addition to factors specific to the patient, choice of the implantation site can affect ease of technical insertion, defibrillation effectiveness, and long-term rates of lead failure.

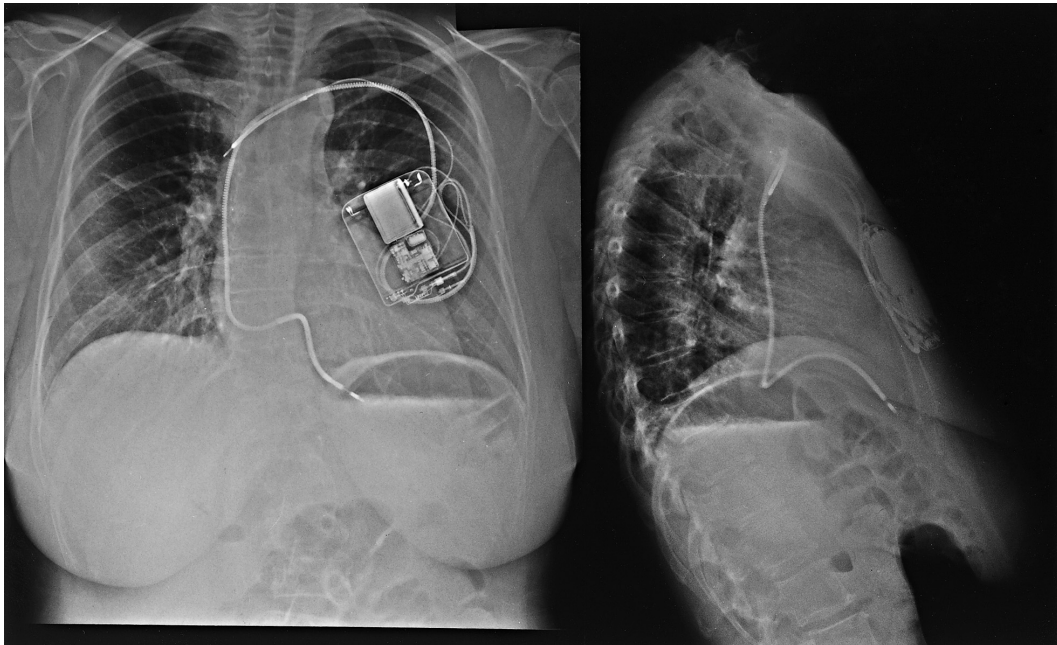


**Fig. 1.36** Chest radiographs depict active pulse generator shell system with an added proximal defibrillation coil to optimize defibrillation threshold.

Right pectoral implantation may be considered in left-handed persons, hunters who place the rifle butt on the left shoulder, and patients with previous mastectomy, other surgical procedures, or anatomy that precludes left-sided insertion. In systems with both distal and proximal defibrillation coils, the proximal coil is either shifted toward the right hemithorax (if both coils are on the same lead) or, often, advanced to a lower superior vena cava position for greater cardiac proximity (in two-lead systems) with right-sided placement. With active can pulse generators, the largest defibrillation lead surface, the device shell, is shifted away from the ventricular myocardium (Fig. 1.37). These unfavorable restrictions on lead position decrease defibrillation effectiveness.<sup>143,144</sup> With biphasic waveforms, we found that right-sided implantation results in a 6-J increase in DFT compared with left-sided placement ( $11.3 \pm 5.3$  J,

left-sided;  $17.0 \pm 4.9$  J, right-sided;  $P < 0.0001$ ).<sup>143</sup> Even with the increase, right-sided devices were successfully placed in 19 of 20 patients; in one patient, an acceptable right-sided threshold could not be achieved and that approach was abandoned. Despite the concern that a right-sided active can might be detrimental by diverting a significant portion of the electrical field away from the ventricles, the large surface area of the shell compensates for this, so that when right-sided implantation is required, active can devices are preferable (Fig. 1.38).<sup>143</sup> In general, however, left-sided insertion is superior to right-sided placement and is used if there are no compelling factors against it.

An alternative site for device placement is the abdomen, but this site is only rarely used. Although not as effective for defibrillation as the left pectoral position, the abdomen appears superior to the right pectoral lo-

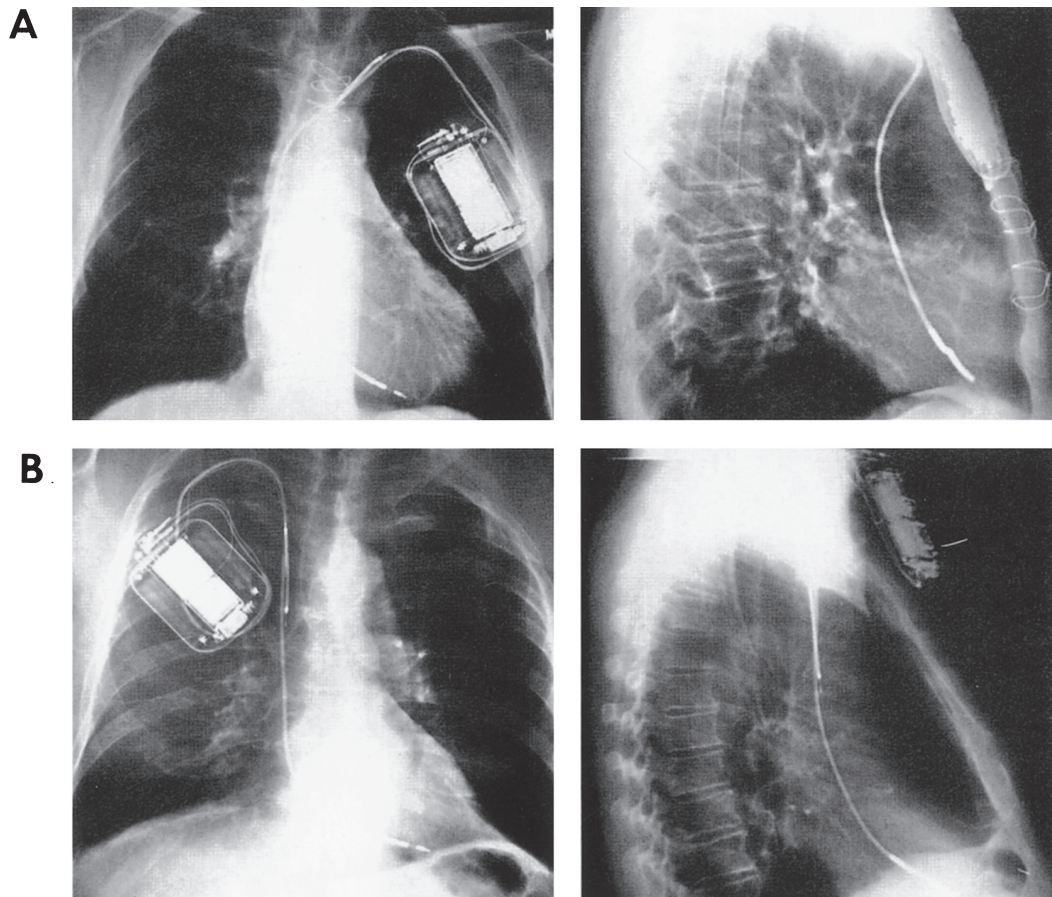


**Fig. 1.37** (A) Posteroanterior and lateral chest radiographs from a patient with a left-sided defibrillator. Note that the proximal defibrillation lead is in the left subclavian vein.

(B) Posteroanterior and lateral chest radiographs from a patient with right-sided defibrillator placement. Note that the proximal defibrillation lead is in the superior vena cava.

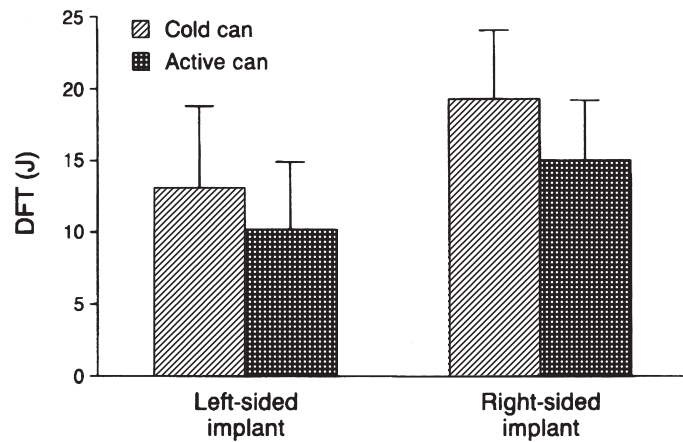


**Fig. 1.38** Defibrillation thresholds with right-sided and left-sided cardioverter-defibrillator implantation of active can and cold can devices. Defibrillation threshold (DFT) is on ordinate, and side of placement and can type are on abscissa. (From Friedman *et al.*<sup>143</sup> By permission of Futura Publishing Company.)

cation for active can placement.<sup>145</sup> However, abdominal insertion is technically more challenging, requiring two incisions, lead tunneling, abdominal dissection (often necessitating surgical assistance), and general anesthesia. Additionally, because of the greater risk of infection, threat of peritoneal erosion and increased risk of lead fracture, even with totally transvenous systems this position is used only in rare circumstances.<sup>146</sup>

### Drugs and defibrillators

Antiarrhythmic agents are frequently used in patients with implantable defibrillators to treat supraventricular arrhythmias (particularly atrial fibrillation), suppress ventricular tachyarrhythmias, and slow VT to increase the responsiveness of antitachycardia pacing. In the implantable defibrillator trials, concomitant use of membrane-active agents (Vaughn-Williams class I or class III drugs) has ranged from 11% to 31%.<sup>147-150</sup> Several important device–drug interactions must be considered.<sup>151</sup>

1. Detection. Most drugs slow VT. If slowed below the detection cut-off rate, VT is not detected by the device and remains untreated. Initiation of antiarrhythmic drugs in patients with VT is usually followed by device testing to assess detection of VT.
2. Pacing thresholds. Bradycardia and antitachycardia pacing thresholds may be affected by pharmacological agents, as discussed in Chapter 13.
3. Pacing requirements. Drugs may exacerbate conduction defects or slow the sinus rate, necessitating pacing for bradycardia.
4. Drug-induced proarrhythmia.

5. Changes in DFT. Although it is well known that pharmacological agents can modulate defibrillation effectiveness, drug–defibrillation interactions are complex. Moreover, assessment of the influence of drugs on defibrillation is confounded by the effects of anesthetic agents, variability in lead systems and waveforms across studies, and heterogeneity in study subjects (i.e. human, canine and porcine). In general, however, agents that impede the fast inward sodium current (such as lidocaine) or calcium channel function (such as verapamil) increase the DFT, whereas agents that block repolarizing potassium currents (such as sotalol) lower the DFT. The effects of amiodarone are legion; clinically, long-term administration of amiodarone increases DFTs, whereas intravenous administration has little immediate effect. In addition to antiarrhythmic agents, other drugs have been shown to increase the defibrillation threshold, such as sildenafil<sup>152</sup>, venlafaxine<sup>153</sup> and alcohol<sup>154</sup>.

Importantly, with current generation biphasic ICDs, the clinical effect of most drugs, including amiodarone, is modest.<sup>155</sup> In general, then, ICD evaluation should be performed when administration of membrane active drugs that can increase the threshold (especially amiodarone) is initiated, particularly in patients with borderline DFTs. Drug effects on defibrillation are summarized in Table 1.4. In patients with a low DFT, testing for slow VTs or, less commonly, empirically lengthening the detection interval (to allow for VT slowing) is most important. As a general rule, ICD evaluation should be considered whenever administration of Vaughn-Williams class I or class III drugs is initiated or their dosage significantly increased. These drugs are listed

<i>Drug</i>	<i>Class</i> <sup>*</sup>	<i>Effect on defibrillation threshold</i> <sup>†</sup>
Quinidine	IA	Increase
Procainamide	IA	No change
N-acetylprocainamide	IA	Decrease
Disopyramide	IA	No change
Mexiletine	IB	Increase
Flecainide	IC	Increase
Moricizine	IC	Increase
Propafenone	IC	No change
Propranolol	II	Increase
Atenolol	II	No change
Isoproterenol		Decrease
Sotalol	III	Decrease
Ibutilide	III	Decrease
Dofetilide	III	Decrease
Amiodarone	III	
Oral		Increase
Intravenous		No change or decrease
Diltiazem	IV	Increase
Verapamil	IV	Increase

**Table 1.4** Effects of drugs on defibrillation

\*Vaughn-Williams classification.

†If study results conflict, the most frequently reported effect is noted.

Modified from Carnes *et al.*<sup>151</sup> By permission of Pharmacotherapy Publications.

in Table 1.5. Drug and defibrillator interactions are also discussed in Chapter 13.

It is equally important to remember that use of cardiovascular medications outside of membrane active drugs (i.e. use of ACE-inhibitors, angiotensin receptor blockers,  $\beta$ -blockers, statins, aspirin, warfarin, and other evidence-based medications have been shown to reduce mortality in various clinical situations) does not interact with ICD function in any clinically significant way, and should therefore be encouraged.

## References

- Hodgkin A, Huxley A. Quantitative description of membrane current and its application to conduction and excitation in nerve. *J Physiol (Lond)* 1952; 117:500–44.
- Gadsby DC. The Na/K pump of cardiac cells. *Annu Rev Biophys Bioeng* 1984; 13:373–98.
- Glitsch HG. Electrogenic Na pumping in the heart. *Annu Rev Physiol* 1982; 44:389–400.
- Balser JR. Structure and function of the cardiac sodium channels. *Cardiovasc Res* 1999; 42:327–38.

<i>Vaughn-Williams classification</i>	<i>Medication</i>
IA	Quinidine, procainamide, disopyramide
IB	Lidocaine, tocainide, phenytoin
IC	Flecainide, propafenone, encainide, moricizine
III	Sotalol, ibutilide, dofetilide, amiodarone

**Table 1.5** Membrane-active drugs<sup>\*</sup>

\*These agents may significantly affect defibrillator function, often mandating device testing on initiation.

- 5 Makielski JC, Sheets MF, Hanck DA, January CT, Fozzard HA. Sodium current in voltage clamped internally perfused canine cardiac Purkinje cells. *Biophys J* 1987; 52:1–11.
- 6 Kunze DL, Lacerda AE, Wilson DL, Brown AM. Cardiac Na currents and the inactivating, reopening, and waiting properties of single cardiac Na channels. *J Gen Physiol* 1985; 86:691–719.
- 7 Cohen CJ, Bean BP, Tsien RW. Maximal upstroke velocity as an index of available sodium conductance. Comparison of maximal upstroke velocity and voltage clamp measurements of sodium current in rabbit Purkinje fibers. *Circ Res* 1984; 54:636–51.
- 8 Hume JR, Giles W. Ionic currents in single isolated bullfrog atrial cells. *J Gen Physiol* 1983; 81:153–94.
- 9 Reuter H. Divalent cations as charge carriers in excitable membranes. *Prog Biophys Mol Biol* 1973; 26:1–43.
- 10 Hume JR, Giles W, Robinson K *et al.* A time- and voltage-dependent K<sup>+</sup> current in single cardiac cells from bullfrog atrium. *J Gen Physiol* 1986; 88:777–98.
- 11 Barr L, Dewey MM, Berger W. Propagation of action potentials and the structure of the nexus in cardiac muscle. *J Gen Physiol* 1965; 48:797–823.
- 12 De Mello WC. Intercellular communication in cardiac muscle. *Circ Res* 1982; 51:1–9.
- 13 Barold SS, Ong LS, Heinle RA. Stimulation and sensing thresholds for cardiac pacing: electrophysiologic and technical aspects. *Prog Cardiovasc Dis* 1981; 24:1–24.
- 14 Lindemans FW, Denier Van der Gon JJ. Current thresholds and liminal size in excitation of heart muscle. *Cardiovasc Res* 1978; 12:477–85.
- 15 de Voogt WG. Pacemaker leads: performance and progress. *Am J Cardiol* 1999; 83:187D–191D.
- 16 Timmis G, Helland J, Westveer D. The evolution of low threshold leads. *Clin Prog Pacing Electrophysiol* 1983; 1:313–34.
- 17 Kay GN, Anderson K, Epstein AE, Plumb VJ. Active fixation atrial leads: randomized comparison of two lead designs. *Pacing Clin Electrophysiol* 1989; 12:1355–61.
- 18 de Buitelir M, Kou WH, Schmaltz S, Morady F. Acute changes in pacing threshold and R- or P-wave amplitude during permanent pacemaker implantation. *Am J Cardiol* 1990; 65:999–1003.
- 19 Kruse IM, Terpstra B. Acute and long-term atrial and ventricular stimulation thresholds with a steroid-eluting electrode. *Pacing Clin Electrophysiol* 1985; 8:45–9.
- 20 Mond H, Stokes K, Helland J *et al.* The porous titanium steroid eluting electrode: a double blind study assessing the stimulation threshold effects of steroid. *Pacing Clin Electrophysiol* 1988; 11:214–9.
- 21 Guarda F, Galloni M, Assone F, Pasteris V, Luboz MP. Histological reactions of porous tip endocardial electrodes implanted in sheep. *Int J Artif Organs* 1982; 5:267–73.
- 22 Beyersdorf F, Schneider M, Kreuzer J, Falk S, Zegelman M, Satter P. Studies of the tissue reaction induced by transvenous pacemaker electrodes. I. Microscopic examination of the extent of connective tissue around the electrode tip in the human right ventricle. *Pacing Clin Electrophysiol* 1988; 11:1753–9.
- 23 Schwaab B, Frohlig G, Berg M, Schwerdt H, Schieffer H. Five-year follow-up of a bipolar steroid-eluting ventricular pacing lead. *Pacing Clin Electrophysiol* 1999; 22:1226–8.
- 24 Wiegand UK, Potratz J, Bonnemeier H *et al.* Long-term superiority of steroid elution in atrial active fixation platinum leads. *Pacing Clin Electrophysiol* 2000; 23:1003–9.
- 25 Klein HH, Steinberger J, Knake W. Stimulation characteristics of a steroid-eluting electrode compared with three conventional electrodes. *Pacing Clin Electrophysiol* 1990; 13:134–7.
- 26 King DH, Gillette PC, Shannon C, Cuddy TE. Steroid-eluting endocardial pacing lead for treatment of exit block. *Am Heart J* 1983; 106:1438–40.
- 27 Furman S, Hurzeler P, DeCaprio V. The ventricular endocardial electrogram and pacemaker sensing. *J Thorac Cardiovasc Surg* 1977; 73:258–66.
- 28 Kleinert M, Elmqvist H, Strandberg H. Spectral properties of atrial and ventricular endocardial signals. *Pacing Clin Electrophysiol* 1979; 2:11–9.
- 29 Watson W. Myopotential sensing in cardiac pacemakers. In: Barold SS, ed. *Modern cardiac pacing*. Mount Kisco, NY: Futura Publishing Co., 1985:813–37.
- 30 Parsonnet V, Myers GH, Kresh YM. Characteristics of intracardiac electrograms II: Atrial endocardial electrograms. *Pacing Clin Electrophysiol* 1980; 3:406–17.
- 31 Hurzeler P, De Caprio V, Furman S. Endocardial electrograms and pacemaker sensing. *Med Instrum* 1976; 10:178–82.
- 32 Sweesy MW, Batey RL, Forney RC. Crosstalk during bipolar pacing. *Pacing Clin Electrophysiol* 1988; 11:1512–6.
- 33 Janosik DL, Redd RM, Kennedy HL. Crosstalk inhibition of a dual-chamber pacemaker diagnosed by ambulatory electrocardiography. *Am Heart J* 1990; 120:435–8.
- 34 Clarke M, Liu B, Schuller H *et al.* Automatic adjustment of pacemaker stimulation output correlated with continuously monitored capture thresholds: a multicenter study. European Microny Study Group. *Pacing Clin Electrophysiol* 1998; 21:1567–75.
- 35 Kay GN. Basic aspects of cardiac pacing. In: Ellenbogen K, ed. *Cardiac pacing*. Boston: Blackwell Scientific Publications, 1992:32–119.
- 36 Raymond RD, Nanian KB. Insulation failure with bipolar polyurethane pacing leads. *Pacing Clin Electrophysiol* 1984; 7:378–80.

- 37 Bornzin G. A low threshold, low polarization platinumized endocardial electrode (abstract). *Pacing Clin Electrophysiol* 1983; 6:A-70.
- 38 Kertes P, Mond H, Sloman G, Vohra J, Hunt D. Comparison of lead complications with polyurethane tined, silicone rubber tined, and wedge tip leads: clinical experience with 822 ventricular endocardial leads. *Pacing Clin Electrophysiol* 1983; 6:957-62.
- 39 Hanson JS. Sixteen failures in a single model of bipolar polyurethane-insulated ventricular pacing lead: a 44-month experience. *Pacing Clin Electrophysiol* 1984; 7:389-94.
- 40 Mond HG, Grenz D. Implantable transvenous pacing leads: the shape of things to come. *Pacing Clin Electrophysiol* 2004; 27:887-93.
- 41 Calfee RV, Saulson SH. A voluntary standard for 3.2 mm unipolar and bipolar pacemaker leads and connectors. *Pacing Clin Electrophysiol* 1986; 9:1181-5.
- 42 Rho RW, Patel VV, Gerstenfeld EP *et al*. Elevations in ventricular pacing threshold with the use of the Y adaptor: implications for biventricular pacing. *Pacing Clin Electrophysiol* 2003; 26:747-51.
- 43 Taieb JM, Barnay C, Linde C, Mortensen P, Menardis M. Left atrial far-field sensing by left ventricular leads: a potential hazard in cardiac resynchronization therapy. *Europace* 2005; 7:611-6.
- 44 Mond HG. Unipolar versus bipolar pacing—poles apart. *Pacing Clin Electrophysiol* 1991; 14:1411-24.
- 45 Gregoratos G, Abrams J, Epstein AE *et al*. ACC/AHA/NASPE 2002 guideline update for implantation of cardiac pacemakers and antiarrhythmia devices: summary article. A report of the American College of Cardiology/American Heart Association Task Force on Practice Guidelines (ACC/AHA/NASPE Committee to Update the 1998 Pacemaker Guidelines). *J Cardiovasc Electrophysiol* 2002; 13:1183-99.
- 46 Abraham WT, Hayes DL. Cardiac resynchronization therapy for heart failure. *Circulation* 2003; 108:2596-603.
- 47 Sogaard P, Egeblad H, Kim WY *et al*. Tissue Doppler imaging predicts improved systolic performance and reversed left ventricular remodeling during long-term cardiac resynchronization therapy. *J Am Coll Cardiol* 2002; 40:723-30.
- 48 Wilkoff BL, Belott PH, Love CJ *et al*. Improved extraction of ePTFE and medical adhesive modified defibrillation leads from the coronary sinus and great cardiac vein. *Pacing Clin Electrophysiol* 2005; 28:205-11.
- 49 Furman S. Basic concepts. In: Furman S, Hayes DL, Holmes DR, eds. *A practice of cardiac pacing*. Mount Kisco, NY: Futura Publishing Co., 1993:29-88.
- 50 Schoenfeld MH. Contemporary pacemaker and defibrillator device therapy: challenges confronting the general cardiologist. *Circulation* 2007; 115:638-53.
- 51 Ribeiro AL, Rincon LG, Oliveira BG *et al*. Automatic adjustment of pacing output in the clinical setting. *Am Heart J* 2004; 147:127-31.
- 52 Tyers GF, Brownlee RR. Power pulse generators, electrodes, and longevity. *Prog Cardiovasc Dis* 1981; 23:421-34.
- 53 Irnich W. Muscle noise and interference behavior in pacemakers: a comparative study. *Pacing Clin Electrophysiol* 1987; 10:125-32.
- 54 Bicik V, Kristan L. Sine2/triangle/square wave generator for pacemaker testing. *Pacing Clin Electrophysiol* 1985; 8:484-93.
- 55 Hauser RG, Kallinen L. Deaths associated with implantable cardioverter defibrillator failure and deactivation reported in the United States Food and Drug Administration Manufacturer and User Facility Device Experience Database. *Heart Rhythm* 2004; 1:399-405.
- 56 Zaim S, Sunthorn H, Adatte JJ, Kursteiner K, Burgener D, Huehn C. Inappropriate high-rate ventricular pacing in a patient with a defibrillator. *Europace* 2002; 4:427-30.
- 57 Bernstein AD, Daubert JC, Fletcher RD *et al*. The revised NASPE/BPEG generic code for antibradycardia, adaptive-rate, and multisite pacing. North American Society of Pacing and Electrophysiology/British Pacing and Electrophysiology Group. *Pacing Clin Electrophysiol* 2002; 25:260-4.
- 58 Prevost J, Battelli F. Some effects of electrical discharge on the hearts of mammals. *Comptes Rendus Acad Sci* 1899; 129:1267-8.
- 59 Weiss JN, Qu Z, Chen PS *et al*. The dynamics of cardiac fibrillation. *Circulation* 2005; 112:1232-40.
- 60 Gurvich N, Yuniev G. Restoration of regular rhythm in mammalian fibrillating heart. *Am Rev Soviet Med* 1946; 3:236-9.
- 61 Zipes DP, Fischer J, King RM, Nicoll Ad, Jolly WW. Termination of ventricular fibrillation in dogs by depolarizing a critical amount of myocardium. *Am J Cardiol* 1975; 36:37-44.
- 62 Chen PS, Shibata N, Dixon EG *et al*. Activation during ventricular defibrillation in open-chest dogs. Evidence of complete cessation and regeneration of ventricular fibrillation after unsuccessful shocks. *J Clin Invest* 1986; 77:810-23.
- 63 Chen PS, Wolf PD, Melnick SD, Danieley ND, Smith WM, Ideker RE. Comparison of activation during ventricular fibrillation and following unsuccessful defibrillation shocks in open-chest dogs. *Circ Res* 1990; 66:1544-60.
- 64 Frazier DW, Wolf PD, Wharton JM, Tang AS, Smith WM, Ideker RE. Stimulus-induced critical point. Mechanism for electrical initiation of reentry in normal canine myocardium. *J Clin Invest* 1989; 83:1039-52.

- 65 Swerdlow CD, Martin DJ, Kass RM *et al.* The zone of vulnerability to T wave shocks in humans. *J Cardiovasc Electrophysiol* 1997; 8:145–54.
- 66 Chen PS, Feld GK, Kriett JM *et al.* Relation between upper limit of vulnerability and defibrillation threshold in humans. *Circulation* 1993; 88:186–92.
- 67 Dillon SM, Kwaku KF. Progressive depolarization: a unified hypothesis for defibrillation and fibrillation induction by shocks. *J Cardiovasc Electrophysiol* 1998; 9:529–52.
- 68 Sweeney RJ, Gill RM, Steinberg MI, Reid PR. Ventricular refractory period extension caused by defibrillation shocks. *Circulation* 1990; 82:965–72.
- 69 Dillon SM. The electrophysiological effects of defibrillation shocks. In: Kroll M, Lehmann M, eds. *Implantable cardioverter defibrillator therapy: the engineering–clinical interface*. Norwell, MA: Kluwer Academic Publishers, 1996:31–61.
- 70 Kroll MW, Efimov IR, Tchou PJ. Present understanding of shock polarity for internal defibrillation: the obvious and non-obvious clinical implications. *Pacing Clin Electrophysiol* 2006; 29:885–91.
- 71 Yamanouchi Y, Cheng Y, Tchou PJ, Efimov IR. The mechanisms of the vulnerable window: the role of virtual electrodes and shock polarity. *Can J Physiol Pharmacol* 2001; 79:25–33.
- 72 Efimov IR, Cheng Y, Yamanouchi Y, Tchou PJ. Direct evidence of the role of virtual electrode-induced phase singularity in success and failure of defibrillation. *J Cardiovasc Electrophysiol* 2000; 11:861–8.
- 73 Luceri RM, Habal SM, David IB, Puchferran RL, Muratore C, Rabinovich R. Changing trends in therapy delivery with a third generation noncommitted implantable defibrillator: results of a large single center clinical trial. *Pacing Clin Electrophysiol* 1993; 16:159–64.
- 74 Wathen MS, DeGroot PJ, Sweeney MO *et al.* Prospective randomized multicenter trial of empirical antitachycardia pacing versus shocks for spontaneous rapid ventricular tachycardia in patients with implantable cardioverter-defibrillators: Pacing Fast Ventricular Tachycardia Reduces Shock Therapies (PainFREE Rx II) trial results. *Circulation* 2004; 110:2591–6.
- 75 Israel CW, Hugl B, Unterberg C *et al.* Pace-termination and pacing for prevention of atrial tachyarrhythmias: results from a multicenter study with an implantable device for atrial therapy. *J Cardiovasc Electrophysiol* 2001; 12:1121–8.
- 76 Gillis AM, Morck M. Atrial fibrillation after DDDR pacemaker implantation. *J Cardiovasc Electrophysiol* 2002; 13:542–7.
- 77 Gillis AM, Koehler J, Morck M, Mehra R, Hettrick DA. High atrial antitachycardia pacing therapy efficacy is associated with a reduction in atrial tachyarrhythmia burden in a subset of patients with sinus node dysfunction and paroxysmal atrial fibrillation. *Heart Rhythm* 2005; 2:791–6.
- 78 Adler SW 2nd, Wolpert C, Warman EN, Musley SK, Koehler JL, Euler DE. Efficacy of pacing therapies for treating atrial tachyarrhythmias in patients with ventricular arrhythmias receiving a dual-chamber implantable cardioverter defibrillator. *Circulation* 2001; 104:887–92.
- 79 Friedman PA, Dijkman B, Warman EN *et al.* Atrial therapies reduce atrial arrhythmia burden in defibrillator patients. *Circulation* 2001; 104:1023–8.
- 80 Lau CP. Pacing for atrial fibrillation. *Heart* 2003; 89:106–12.
- 81 Ripplinger CM, Krinsky VI, Nikolski VP, Efimov IR. Mechanisms of unpinning and termination of ventricular tachycardia. *Am J Physiol Heart Circ Physiol* 2006; 291:H184–92.
- 82 Wathen M, Yee R, Birgersdotter-Green U, Belk P, Christensen J, Jackson T. The influence of antitachycardia pacing site on efficacy of ventricular tachycardia termination. *Circulation* 2004; 110:III-443 (Abstract).
- 83 Byrd IA, Rogers JM, Smith WM, Pollard AE. Comparison of conventional and biventricular antitachycardia pacing in a geometrically realistic model of the rabbit ventricle. *J Cardiovasc Electrophysiol* 2004; 15:1066–77.
- 84 Kuhlkamp V. Initial experience with an implantable cardioverter-defibrillator incorporating cardiac resynchronization therapy. *J Am Coll Cardiol* 2002; 39:790–7.
- 85 Young JB, Abraham WT, Smith AL *et al.* Combined cardiac resynchronization and implantable cardioversion defibrillation in advanced chronic heart failure: the MIRACLE ICD Trial. *JAMA* 2003; 289:2685–94.
- 86 Schwab JO, Gasparini M, Anselme F *et al.* Right ventricular versus biventricular antitachycardia pacing in the termination of ventricular tachyarrhythmia in patients receiving cardiac resynchronization therapy: the ADVANCE CRT-D trial. *J Cardiovasc Electrophysiol* 2006; 17:504–7.
- 87 Takagi S, Pumir A, Pazo D, Efimov I, Nikolski V, Krinsky V. Unpinning and removal of a rotating wave in cardiac muscle. *Phys Rev Lett* 2004; 93:058101.
- 88 Strickberger SA, Daoud EG, Davidson T *et al.* Probability of successful defibrillation at multiples of the defibrillation energy requirement in patients with an implantable defibrillator. *Circulation* 1997; 96:1217–23.
- 89 Davy JM, Fain ES, Dorian P, Winkle RA. The relationship between successful defibrillation and delivered energy in open-chest dogs: reappraisal of the “defibrillation threshold” concept. *Am Heart J* 1987; 113:77–84.
- 90 Brady PA, Friedman PA, Stanton MS. Effect of failed defibrillation shocks on electrogram amplitude in a non-integrated transvenous defibrillation lead system. *Am J Cardiol* 1995; 76:580–4.

- 91 Ideker RE, Hillsley RE, Wharton JM. Shock strength for the implantable defibrillator: can you have too much of a good thing? *Pacing Clin Electrophysiol* 1992; 15:841–4.
- 92 Marchlinski FE, Flores B, Miller JM, Gottlieb CD, Hargrove WC 3rd. Relation of the intraoperative defibrillation threshold to successful postoperative defibrillation with an automatic implantable cardioverter defibrillator. *Am J Cardiol* 1988; 62:393–8.
- 93 Strickberger SA, Man KC, Souza J *et al.* A prospective evaluation of two defibrillation safety margin techniques in patients with low defibrillation energy requirements. *J Cardiovasc Electrophysiol* 1998; 9:41–6.
- 94 Degroot PJ, Church TR, Mehra R, Martinson MS, Schaber DE. Derivation of a defibrillator implant criterion based on probability of successful defibrillation. *Pacing Clin Electrophysiol* 1997; 20:1924–35.
- 95 Luria D, Glikson M, Brady PA *et al.* Predictors and mode of detection of transvenous lead malfunction in implantable defibrillators. *Am J Cardiol* 2001; 87:901–4.
- 96 Gold MR, Higgins S, Klein R *et al.* Efficacy and temporal stability of reduced safety margins for ventricular defibrillation: primary results from the Low Energy Safety Study (LESS). *Circulation* 2002; 105:2043–8.
- 97 Higgins S, Mann D, Calkins H *et al.* One conversion of ventricular fibrillation is adequate for implantable cardioverter-defibrillator implant: an analysis from the Low Energy Safety Study (LESS). *Heart Rhythm* 2005; 2:117–22.
- 98 Gold MR, Breiter D, Leman R, Rashba EJ, Shorofsky SR, Hahn SJ. Safety of a single successful conversion of ventricular fibrillation before the implantation of cardioverter defibrillators. *Pacing Clin Electrophysiol* 2003; 26:483–6.
- 99 Trusty JM, Hayes DL, Stanton MS, Friedman PA. Factors affecting the frequency of subcutaneous lead usage in implantable defibrillators. *Pacing Clin Electrophysiol* 2000; 23:842–6.
- 100 Kettering K, Mewis C, Dornberger V *et al.* Long-term experience with subcutaneous ICD leads: a comparison among three different types of subcutaneous leads. *Pacing Clin Electrophysiol* 2004; 27:1355–61.
- 101 Epstein AE, Ellenbogen KA, Kirk KA, Kay GN, Dailey SM, Plumb VJ. Clinical characteristics and outcome of patients with high defibrillation thresholds. A multicenter study. *Circulation* 1992; 86:1206–16.
- 102 Watanabe H, Chinushi M, Sugiura H *et al.* Unsuccessful internal defibrillation in Brugada syndrome: focus on refractoriness and ventricular fibrillation cycle length. *J Cardiovasc Electrophysiol* 2005; 16:262–6.
- 103 Venditti FJ Jr, John RM, Hull M, Tofler GH, Shahian DM, Martin DT. Circadian variation in defibrillation energy requirements. *Circulation* 1996; 94:1607–12.
- 104 Russo AM, Sauer W, Gerstenfeld EP *et al.* Defibrillation threshold testing: is it really necessary at the time of implantable cardioverter-defibrillator insertion? *Heart Rhythm* 2005; 2:456–61.
- 105 Ideker RE, Epstein AE, Plumb VJ. Should shocks still be administered during implantable cardioverter-defibrillator insertion? *Heart Rhythm* 2005; 2:462–3.
- 106 Swerdlow CD, Russo AM, Degroot PJ. The dilemma of ICD implant testing. *Pacing Clin Electrophysiol* 2007; 30:675–700.
- 107 Glikson M, Gurevitz OT, Trusty JM *et al.* Upper limit of vulnerability determination during implantable cardioverter-defibrillator placement to minimize ventricular fibrillation inductions. *Am J Cardiol* 2004; 94:1445–9.
- 108 Hwang C, Swerdlow CD, Kass RM *et al.* Upper limit of vulnerability reliably predicts the defibrillation threshold in humans. *Circulation* 1994; 90:2308–14.
- 109 Chen PS, Shibata N, Dixon EG, Martin RO, Ideker RE. Comparison of the defibrillation threshold and the upper limit of ventricular vulnerability. *Circulation* 1986; 73:1022–8.
- 110 Behrens S, Li C, Franz MR. Effects of myocardial ischemia on ventricular fibrillation inducibility and defibrillation efficacy. *J Am Coll Cardiol* 1997; 29:817–24.
- 111 Swerdlow CD, Peter CT, Kass RM *et al.* Programming of implantable cardioverter-defibrillators on the basis of the upper limit of vulnerability. *Circulation* 1997; 95:1497–504.
- 112 Swerdlow CD, Ahern T, Kass RM, Davie S, Mandel WJ, Chen PS. Upper limit of vulnerability is a good estimator of shock strength associated with 90% probability of successful defibrillation in humans with transvenous implantable cardioverter-defibrillators. *J Am Coll Cardiol* 1996; 27:1112–8.
- 113 Rodriguez B, Tice BM, Eason JC, Aguel F, Ferrero JM Jr, Trayanova N. Effect of acute global ischemia on the upper limit of vulnerability: a simulation study. *Am J Physiol Heart Circ Physiol* 2004; 286:H2078–88.
- 114 Gurevitz OT, Friedman PA, Glikson M *et al.* Discrepancies between the upper limit of vulnerability and defibrillation threshold: prevalence and clinical predictors. *J Cardiovasc Electrophysiol* 2003; 14:728–32.
- 115 Schuder JC, Gold JH, Stoeckle H, Granberg TA, Dettmer JC, Larwill MH. Transthoracic ventricular defibrillation in the 100 kg calf with untruncated and truncated exponential stimuli. *IEEE Trans Biomed Eng* 1980; 27:37–43.
- 116 Shorofsky SR, Rashba E, Havel W *et al.* Improved defibrillation efficacy with an ascending ramp waveform in humans. *Heart Rhythm* 2005; 2:388–94.
- 117 Olsovsky MR, Hodgson DM, Shorofsky SR, Kavesh NG, Gold MR. Effect of biphasic waveforms on transvenous defibrillation thresholds in patients with coronary artery disease. *Am J Cardiol* 1997; 80:1098–100.



- 118 Wyse DG, Kavanagh KM, Gillis AM *et al.* Comparison of biphasic and monophasic shocks for defibrillation using a nonthoracotomy system. *Am J Cardiol* 1993; 71:197–202.
- 119 Bardy GH, Ivey TD, Allen MD, Johnson G, Mehra R, Greene HL. A prospective randomized evaluation of biphasic versus monophasic waveform pulses on defibrillation efficacy in humans. *J Am Coll Cardiol* 1989; 14:728–33.
- 120 Jones JL, Swartz JF, Jones RE, Fletcher R. Increasing fibrillation duration enhances relative asymmetrical biphasic versus monophasic defibrillator waveform efficacy. *Circ Res* 1990; 67:376–84.
- 121 Schuder JC, McDaniel WC, Stoeckle H. Defibrillation of 100 kg calves with asymmetrical, bidirectional, rectangular pulses. *Cardiovasc Res* 1984; 18:419–26.
- 122 Kavanagh KM, Tang AS, Rollins DL, Smith WM, Ideker RE. Comparison of the internal defibrillation thresholds for monophasic and double and single capacitor biphasic waveforms. *J Am Coll Cardiol* 1989; 14:1343–9.
- 123 Fain ES, Sweeney MB, Franz MR. Improved internal defibrillation efficacy with a biphasic waveform. *Am Heart J* 1989; 117:358–64.
- 124 Denman RA, Umesan C, Martin PT *et al.* Benefit of millisecond waveform durations for patients with high defibrillation thresholds. *Heart Rhythm* 2006; 3:536–41.
- 125 Natarajan S, Henthorn R, Burroughs J *et al.* “Tuned” defibrillation waveforms outperform 50/50% tilt defibrillation waveforms: a randomized multi-center study. *Pacing Clin Electrophysiol* 2007; 30 (Suppl. 1):S139–42.
- 126 Strickberger SA, Hummel JD, Horwood LE *et al.* Effect of shock polarity on ventricular defibrillation threshold using a transvenous lead system. *J Am Coll Cardiol* 1994; 24:1069–72.
- 127 Bardy GH, Ivey TD, Allen MD, Johnson G, Greene HL. Evaluation of electrode polarity on defibrillation efficacy. *Am J Cardiol* 1989; 63:433–7.
- 128 Natale A, Sra J, Dhala A *et al.* Effects of initial polarity on defibrillation threshold with biphasic pulses. *Pacing Clin Electrophysiol* 1995; 18:1889–93.
- 129 Strickberger SA, Man KC, Daoud E *et al.* Effect of first-phase polarity of biphasic shocks on defibrillation threshold with a single transvenous lead system. *J Am Coll Cardiol* 1995; 25:1605–8.
- 130 Olsovsky MR, Shorofsky SR, Gold MR. Effect of shock polarity on biphasic defibrillation thresholds using an active pectoral lead system. *J Cardiovasc Electrophysiol* 1998; 9:350–4.
- 131 Sweeney RJ, Gill RM, Jones JL, Reid PR. Defibrillation using a high-frequency series of monophasic rectangular pulses: observations and model predictions. *J Cardiovasc Electrophysiol* 1996; 7:134–43.
- 132 Fishler MG. Theoretical predictions of the optimal monophasic and biphasic defibrillation waveshapes. *IEEE Trans Biomed Eng* 2000; 47:59–67.
- 133 Kladner RD. An optimally energized cardiac pacemaker. *IEEE Trans Biomed Eng* 1973; 20:350–6.
- 134 Hillsley RE, Walker RG, Swanson DK *et al.* Is the second phase of a biphasic defibrillation waveform the defibrillating phase? *Pacing Clin Electrophysiol* 1993; 16:1401–11.
- 135 Zhou X, Smith WM, Justice RK, Wayland JL, Ideker RE. Transmembrane potential changes caused by monophasic and biphasic shocks. *Am J Physiol* 1998; 275:H1798–807.
- 136 Tang AS, Yabe S, Wharton JM, Dolker M, Smith WM, Ideker RE. Ventricular defibrillation using biphasic waveforms: the importance of phasic duration. *J Am Coll Cardiol* 1989; 13:207–14.
- 137 Jones JL, Jones RE. Decreased defibrillator-induced dysfunction with biphasic rectangular waveforms. *Am J Physiol* 1984; 247:H792–6.
- 138 Ideker RE, Wolf PD, Alferness C, Krassowska W, Smith WM. Current concepts for selecting the location, size and shape of defibrillation electrodes. *Pacing Clin Electrophysiol* 1991; 14:227–40.
- 139 Gold MR, Foster AH, Shorofsky SR. Lead system optimization for transvenous defibrillation. *Am J Cardiol* 1997; 80:1163–7.
- 140 Bardy GH, Dolack GL, Kudenchuk PJ, Poole JE, Mehra R, Johnson G. Prospective, randomized comparison in humans of a unipolar defibrillation system with that using an additional superior vena cava electrode. *Circulation* 1994; 89:1090–3.
- 141 Winter J, Heil JE, Schumann C *et al.* Effect of implantable cardioverter/defibrillator lead placement in the right ventricle on defibrillation energy requirements. A combined experimental and clinical study. *Eur J Cardiothorac Surg* 1998; 14:419–25.
- 142 Gold MR, Olsovsky MR, DeGroot PJ, Cuello C, Shorofsky SR. Optimization of transvenous coil position for active can defibrillation thresholds. *J Cardiovasc Electrophysiol* 2000; 11:25–9.
- 143 Friedman PA, Rasmussen MJ, Grice S, Trusty J, Glikson M, Stanton MS. Defibrillation thresholds are increased by right-sided implantation of totally transvenous implantable cardioverter defibrillators. *Pacing Clin Electrophysiol* 1999; 22:1186–92.
- 144 Epstein AE, Kay GN, Plumb VJ, Voshage-Stahl L, Hull ML. Elevated defibrillation threshold when right-sided venous access is used for nonthoracotomy implantable defibrillator lead implantation. The Endotak Investigators. *J Cardiovasc Electrophysiol* 1995; 6:979–86.
- 145 Heil JE, Lin Y, Derfus DL, Lang DJ. Impact of ICD electrode position on transvenous defibrillation thresholds. *Pacing Clin Electrophysiol* 1995; 18:873 (Abstract).

- 146 Brady PA, Friedman PA, Trusty JM, Grice S, Hammill SC, Stanton MS. High failure rate for an epicardial implantable cardioverter-defibrillator lead: implications for long-term follow-up of patients with an implantable cardioverter-defibrillator. *J Am Coll Cardiol* 1998; 31:616–22.
- 147 Buxton AE, Lee KL, DiCarlo L *et al*. Electrophysiologic testing to identify patients with coronary artery disease who are at risk for sudden death. Multicenter Unsustained Tachycardia Trial Investigators. *N Engl J Med* 2000; 342:1937–45.
- 148 Bardy GH, Lee KL, Mark DB *et al*. Amiodarone or an implantable cardioverter-defibrillator for congestive heart failure. *N Engl J Med* 2005; 352:225–37.
- 149 The Antiarrhythmics versus Implantable Defibrillators (AVID) Investigators. A comparison of antiarrhythmic-drug therapy with implantable defibrillators in patients resuscitated from near-fatal ventricular arrhythmias. *N Engl J Med* 1997; 337:1576–83.
- 150 Moss AJ, Zareba W, Hall WJ *et al*. Prophylactic implantation of a defibrillator in patients with myocardial infarction and reduced ejection fraction. *N Engl J Med* 2002; 346:877–83.
- 151 Carnes CA, Mehdiraz AA, Nelson SD. Drug and defibrillator interactions. *Pharmacotherapy* 1998; 18:516–25.
- 152 Shinlapawittayatorn K, Sungnoon R, Chattipakorn S, Chattipakorn N. Effects of sildenafil citrate on defibrillation efficacy. *J Cardiovasc Electrophysiol* 2006; 17:292–5.
- 153 Carnes CA, Pickworth KK, Votolato NA, Raman SV. Elevated defibrillation threshold with venlafaxine therapy. *Pharmacotherapy* 2004; 24:1095–8.
- 154 Papaioannou GI, Kluger J. Ineffective ICD therapy due to excessive alcohol and exercise. *Pacing Clin Electrophysiol* 2002; 25:1144–5.
- 155 Hohnloser SH, Dorian P, Roberts R *et al*. Effect of amiodarone and sotalol on ventricular defibrillation threshold: the optimal pharmacological therapy in cardioverter defibrillator patients (OPTIC) trial. *Circulation* 2006; 114:104–9.